

Journal Pre-proof

A continuous coupled hydrological and water resources management model

Alberto Bellin, Bruno Majone, Oscar Cainelli, Daniele Alberici, Francesca Villa

DOI: <http://dx.doi.org/10.1016/j.envsoft.2015.10.013>

Reference: ENSO 3541

To appear in: *Environmental Modelling and Software*

Received date: 10 July 2015

Revised Date: 15 October 2015

Accepted Date: 17 October 2015

Available online Date: 11 November 2015

Please cite this article as: Bellin, A., Majone, B., Cainelli, O., Alberici, D., Villa, F., A continuous coupled hydrological and water resources management model, *Environmental Modelling and Software*, 75, 176-192, 2016, doi: <http://dx.doi.org/10.1016/j.envsoft.2015.10.013>

This is a PDF file of the article accepted for publication by *Environmental Modelling and Software*, but it is not yet the definitive version of record. This version underwent additional copyediting and typesetting before its publication in the final form. Please note that, during the production process, errors may have been discovered which could have affected the content, and all legal disclaimers that apply to the journal pertain. The final version is available at the following journal site:
<http://dx.doi.org/10.1016/j.envsoft.2015.10.013>

A continuous coupled hydrological and water resources management model

Alberto Bellin^{a,*}, Bruno Majone^a, Oscar Cainelli^b, Daniele Alberici^a, Francesca Villa^a

^a*Department of Civil, Environmental and Mechanical Engineering, University of Trento, Via Mesiano 77, I-38123 Trento, Italy*

^b*Smart HydroGeological Solutions Srl, Via Unterveger 52, I-38123 Trento, Italy*

Abstract

Human exploitation of water resources is widespread and its impact on hydrological fluxes is expected to increase in the future. Water use interacts in a complex manner with the hydrological system causing severe alterations of the hydrological fluxes with multifaceted feedbacks. Implementing this coupling within hydrological models is essential when dealing with the impact of human activities on water resources at all relevant scales. We contribute to the effort in developing models coupling natural and human systems with a distributed continuous model, named GEOTRANSF. The model allows to quantify, within the same framework, alterations in the natural regime and constraints and limitations to water resources availability. After presenting GEOTRANSF, an example of application to a medium-size Alpine catchment with streamflow modified by hydropower and distributed uses is discussed, followed by the analysis of the effect of suitable water uses scenarios in the same catchment.

Keywords: hydrological modeling, water resources management, streamflow alterations, hydrological and human systems interactions, scenario-based analyses of water resources

*Corresponding author. Tel.: +39 0461 282637; fax +39 0461 282672.

Email address: alberto.bellin@unitn.it (Alberto Bellin)

Software availability

Name of the software: GEOTRANSF

Developer: Department of Civil, Environmental and Mechanical Engineering, University of Trento, Via Mesiano 77, I-38123 Trento, Italy and Smart HydroGeological Solutions Srl, Via Unterveger 52, I-38123 Trento, Italy.

Contact: Alberto Bellin, Department of Civil, Environmental and Mechanical Engineering, University of Trento, alberto.bellin@unitn.it; Oscar Cainelli, Smart HydroGeological Solutions Srl, oscar.cainelli@smarthydrosol.com.

Hardware: No specific requirements

Software required: FORTRAN compiler

Program Language: FORTRAN

Availability: LGPL licence, source code available upon request to the authors

1. Introduction

Timing and spatial distribution of freshwaters are modified by human intervention almost everywhere in the planet (Sivapalan et al., 2012; Savenije et al., 2014). These modifications are particularly visible in mountain areas due to hydropower exploitation and other distributed uses (i.e., agricultural and industrial, Zolezzi et al., 2009; Botter et al., 2010). A great effort has been devoted in the last decades to gain a better understanding of the processes controlling the terrestrial water cycle, in an attempt to improve hydrological modeling, often focusing on cases with small to negligible human alterations. However, given the widespread relevance of human uses, further effort is needed to gain a better understanding of the interactions between human and hydrological systems (Thompson et al., 2013; Lall, 2014).

Water transfer and storage due to human activities have far reaching implications on the water cycle and water security with feedbacks on climate at local and regional to global scales. For example, intensive agriculture may disturb atmospheric boundary conditions and cause hydroclimatic shifts at a regional scale (see e.g., Destouni et al., 2010, 2013). To address these issues hydrological models should be envisioned that provide full coupling between hydrological process and changes in water fluxes and storage due to human uses. This is particularly relevant for large-scale hydrological models because including water uses at a scale significant and informative for water management is challenging (see e.g., Nazemi and Wheater 2015a,b for a review on the issues and challenges associated to the incorporation of water resources management modules into Earth System Models).

Available models can be classified either as water management-oriented, adopting simplified hydrological kernels (see e.g., IQQM, Simons et al. 1996; MODSIM DSS, Fredericks et al. 1998; RiverWare, Zagona et al. 2001; MFSP, Li et al. 2009) or as hydrological simulation models, which reproduce the relevant hydrological processes with a relatively high level of complexity, but incorporate simplified water management components. Widely used models, such as MIKE SHE (DHI Software, 2009), HEC-HMS (Feldman, 2000) and HSPF (Bicknell et al., 1997; Lampert and Wu, 2015), belong to the latter category, and make use of simplifications in the description of water use and generally ignore dynamic links between natural and human systems. According to Nalbantis et al. (2011) these models can be classified as "monomeric", since they tend to focus on the hydrological component. Holistic models instead, i.e. models in which all parts of the system are simulated with similar details (Nalbantis et al., 2011), as for example RIBASIM (Deltares, 2010), MIKE HYDRO Basin (DHI Software, 2003) and DSF (MRC, 2004), are in general more appealing for operational and planning applications, though their transferability to contexts different from that in which they have been developed may be problematic (see e.g., Dutta et al., 2013).

Source IMS (Welsh et al., 2013), WEAP21 (Yates et al., 2005), SWAT (Neitsh et al., 2011) and HYDROGEIOS (Efstratiadis et al., 2008) are models which integrate hydrological processes and water management rules. In particular, Source IMS and WEAP21 adopt an object-oriented modeling framework in which natural (e.g., runoff and interactions between rivers and groundwater aquifers) and anthropogenic processes (e.g., water demands, reservoirs and river regulation) are conceptualized through the adoption of nodes and transmission links. In both models a conceptual rainfall-runoff module is used to compute water fluxes at selected nodes, at which specific rules are applied to decide amount and timing of water uses. The hydrologic and human-modified systems are in this case loosely coupled, given that uses within the rainfall-runoff areas can be taken into account only by lumping them to the closest node (e.g., Welsh et al., 2013, Fig. 1).

SWAT is a well known model which includes exchanges between hydrological and human systems as source and sink terms, thereby it does take into account feedbacks between the two systems, such as for example the release of water from reservoirs depending in a nonlinear manner from the water elevation. Similarly, HYDROGEIOS is a modeling tool developed to deal with hydrological systems modified by water uses (Efstratiadis et al., 2008). It is based on the concept of Hydrological Response Units (HRUs) (Ross et al., 1979) coupled with a two-compartment bucket model dealing with infiltration and exchanges with atmosphere and groundwater. An interesting feature of this approach is the inclusion of the groundwater component modeled with a network of connected cells. The human component is more sophisticated than in SWAT and it is represented through a linear network programming approach, in which the priorities of conflicting water uses are accounted for through virtual costs. However, the feedback between the two systems is limited to the stream elements and groundwater cells, while it does not include a specific module for flow regulations due to in line storage elements (e.g. reservoirs). The difficulties encountered in modeling the two systems may be alleviated by taking advantage of the services offered by Geographic Information Systems (GIS), as in JGrass-NewAge (Formetta et al., 2011, 2014), though this latter approach does not provide a full coupling between the two systems.

We contribute to this effort by developing a new modeling framework, we called GEOTRANSF, with characteristics similar to HYDROGEIOS and JGrass-NewAge, but with some additional capabilities. The main difference with respect to these tools is a tighter connection between natural and human systems with the inclusion of their feedbacks. For example, withdrawals for irrigation are included as input in the surface bucket representing soil moisture dynamics at the sub-catchment scale. This may be useful in addressing feedbacks between climate change and irrigation, along the lines suggested in the paper by Destouni et al. (2013). Another novelty is represented by the treatment of small diffuse uses from the streams and groundwater, which cannot be treated at the level of the single withdrawal due to their large number and because the cutoff introduced in representing the river network (smaller reaches are not included into the river network, in particular when modeling medium to large catchments). Here, we propose a hierarchical approach, which allows for distribute water uses within the sub-catchment respecting the reciprocal constraints between users along the river network. In our view these are essential features for dealing with all the nonlinear interactions between the hydrological system and the variety of water uses including the effects of the market, in particular the energy market, which influences hydropower production (Seekell et al., 2011; Dalin et al., 2012; Sivapalan et al., 2012).

Water withdrawals along the streams should respect Minimum Environmental Flow (MEF) requirements as part of the objectives indicated in national regulations. Several methodologies have been developed to identify minimal flow conditions that should be respected downstream each withdrawal (see e.g., Acreman et al., 2014). In the simplest case the minimum flow is constant, but modulations to mimic the natural variability, yet with a lower mean, is often applied, particularly in areas of high environmental value. The module of GEOTRANSF dealing with the human component of the water cycle is fully integrated with the natural component and local water budgets are established at intake and restitution points along the river network. For example, withdrawals at a given point of the river network are conditioned to upstream transfers and protocols regulating competing uses, such as the limitations imposed to hydropower by recreational activities and agricultural needs. To the best of our knowledge, these characteristics are not included with a similar level of detail in existing modeling approaches.

In addition, GEOTRANSF can be used to develop scenarios of the human component to be used in impact assessment studies of new water infrastructures, decommissioning of reservoirs and other activities that may be of interest to land and water resources managers. Examples of applications range from the analysis of the impact of future climate and land use scenarios on water resources, to effects of changes in water policies, reservoir storage capacity, irrigation techniques and the overall impact of new run-of-the-river hydropower plants. Within the same framework, the effect of new water policies and possible mitigation actions can be explored and evaluated.

Section 2 describes the hydrological conceptual model, while the model components are described in Section 3. Modeling of human systems is presented in Section 4. Data requirements and parameter identification procedure are presented in Sections 5 and 6, respectively, while two examples of applications are discussed in Section 7. Finally, a set of concluding remarks in Section 8 closes the work.

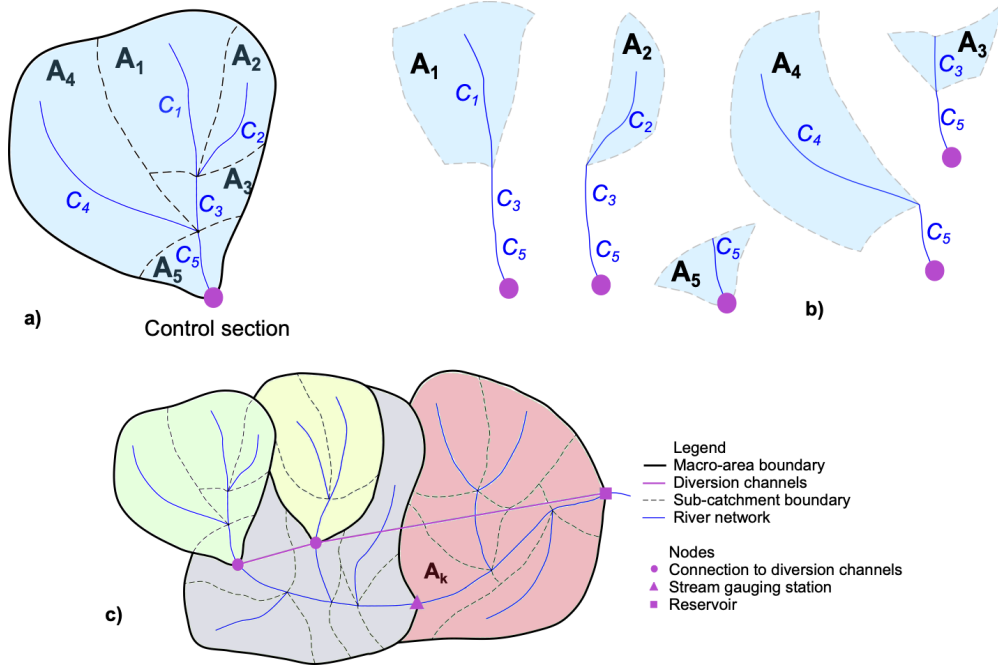


Figure 1: Sketch of GEOTRANSF overall structure: a) the geomorphological structure of a river basin (or a macro area) divided into 5 sub-catchments of area A_i and 5 streams C_i , $i = 1, \dots, 5$. In this simple case, the water discharge at the control section assumes the following general expression: $Q(t) = \sum_{i=1}^5 A_i \int_0^t q_{A_i}(\tau) u_i(t - \tau) d\tau$, where: $u_1(t) = f_{C_1} * f_{C_3} * f_{C_5}$, $u_2(t) = f_{C_2} * f_{C_3} * f_{C_5}$, $u_3(t) = f_{C_3} * f_{C_5}$, $u_4(t) = f_{C_4} * f_{C_5}$, $u_5(t) = f_{C_5}$; b) the collection of pathways available for flow routing towards the control section; c) example of a river basin subdivision into macro-areas identified by a control section (pink node). Each macro-area is evidenced by a different color.

2. Hydrologic system

The model is composed of a hierarchical combination of elements belonging to two morphological units: the sub-catchment and the channel. The former includes the portion of the territory where hillslope processes dominates and the latter is the building block of the river network. The river network is extracted from the Digital Terrain Model (DTM) of the catchment by means of a procedure that first identifies the drainage directions, by either the standard D8 algorithm (O'Callaghan and Mark, 1984) or the improved methods proposed by Tarboton (1997) and Orlandini et al. (2003, 2014), and then classifies the pixels as belonging to a stream or sub-catchment element depending on the value assumed by the parameter: $\tau = \nabla z_i \sqrt{A_i}$, where ∇z_i and A_i are the elevation gradient at the i -th DTM cell and its total contributing area, respectively (e.g. Rodriguez-Iturbe and Rinaldo, 1997; Rinaldo et al., 2006). Pixels with τ larger than an assigned threshold τ_c are classified as streams. The resulting network is composed by interconnected channel elements, each of them with an associated contributing area (sub-catchment) made of the pixels with $\tau < \tau_c$ draining into the pixels of the stream (Fig. 1a). A nonlinear two-component runoff generation model is applied to the sub-catchments. The first component is fast and corresponds to Hortonian excess flow, the second component is slower and represents the sub-surface contribution to the channel into which the sub-catchment drains. The fluxes entering the channel are then transferred to the outlet, or to an intermediate control section, by means of a transfer function given by the convolution of the residence time pdfs of all the channels connected in series from the sub-catchment to the outlet or the control section (see Fig. 1b). Water withdrawals and restitutions due to water uses are also considered as described in Section 4. For example, the contribution originating from the sub-catchment A_1 , $q_{A_1}(t)$ [L/T] is routed to the control section indicated in the Fig. 1a as follows:

$$Q_1(t) = A_1 \int_0^t q_{A_1}(\tau) u_1(t - \tau) d\tau \quad (1)$$

where

$$u_1(t) = f_{C_1} * f_{C_3} * f_{C_5} \quad (2)$$

with f_{C_i} being the residence time pdf of the channel C_i (Rinaldo et al., 2006) and $*$ indicating the convolution operator, i.e. $g_1(t) * g_2(t) = \int_0^t g_1(\tau) g_2(t - \tau) d\tau$, under the assumption that the functions g_1 and g_2 are defined for $t \geq 0$. The contribution from the other sub-catchments can be computed similarly, such that the total water discharge at the control section is given by the sum of all the contributions (see the caption of Fig. 1 for the expression of the total water discharge of the case sketched in Fig. 1 a).

At a higher hierarchical level the river basin is subdivided into several macro-areas, each one identified by a control section. A control section can be one of the following characteristic elements: the outlet of the catchment, a stream gauging station used for calibration, a reservoir, or a section where water is withdrawn from or restituted to the river network (see Fig. 1c). Streamflow computed at a node is transferred to the downstream node or, in the presence of infrastructures, it enters a local water budget equation written by taking into account the characteristics (i.e., water diversion channel, presence of a reservoir, etc.) and constraints of the licensed uses. Water transfer is performed by using the transfer function obtained convolving the pdfs of the sequence of channels connecting the two nodes. Notice that this approach allows flexibility in selecting several control sections within the basin, not necessarily associated with stream-gauging stations.

3. Modules composing the hydrological system

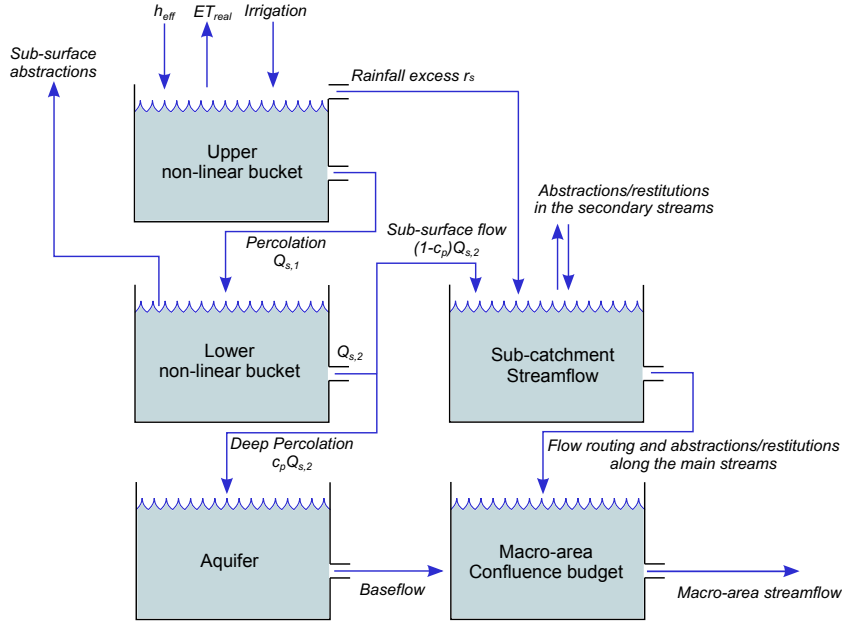
The hydrologic kernel is organized in 4 interconnected modules, which are described in the following and in the Appendices A and B. In particular, Appendix A describes modules dealing with spatialization of precipitation and air temperature measured at the meteorological stations, while Appendix B summarizes modules used for modeling snow dynamics and evapotranspiration, which require the following parameters: the maximum air temperature T_s for precipitation occurring as snow and the minimum air temperature T_{sm} for precipitation occurring as rainfall, the melting rate c_m , in the degree-day snowmelt model, the field capacity θ_{fc} and the residual water content θ_r . The latter are needed in the threshold model for evapotranspiration described in the Appendix B.

3.1. Infiltration, runoff and sub-surface flow

The schematic of the hydrological water balance at the sub-catchment scale is depicted in Fig. 2. Effective rainfall, i.e. rainfall plus snow melting, is separated into infiltration and rainfall excess by means of the following modification of the Soil Conservation Service Curve Number (SCS-CN) model (U.S. Soil Conservation Service, 1964) proposed by Michel et al. (2005):

$$r_s(t) = \begin{cases} \frac{p(t) [\theta(t)b - S_a]}{S^*} \left[2 - \frac{\theta(t)b - S_a}{S^*} \right] & \text{if } \theta(t) > \theta_0 + I_a/b \\ 0, & \text{otherwise} \end{cases} \quad (3)$$

where $p = h_{eff}/\Delta t$ [L/T] is the effective mean rainfall intensity between $t - \Delta t$ and t , r_s [L/T] is the mean runoff rate in the same time interval, θ and θ_0 [L/L] are the actual and initial soil water content, respectively, b [L] is the thickness of the upper soil layer (see the discussion below) and $S_a = I_a + \theta_0 b$ is a modified initial abstraction term. In addition, $S^* = c_s \cdot S$ is the modified maximum potential infiltration, given by the product of the mean S obtained from soil and land use analysis and the calibration parameter c_s . According to Eq. (3) the fraction of the effective rainfall that is transformed into runoff depends on θ , which is continuously updated through mass balance equation (6). Michel et al. (2005) noted that the quantity $S_a = \theta_0 b + I_a$ can be interpreted as a new storage parameter of the model which plays the role of a threshold value above which runoff is generated. In order to simplify the application of the methodology the parameter S_a is assumed to be a fraction of S^* : $S_a = c_a \cdot S^*$, with c_a assumed equal to 0.2, according to the analysis conducted by USGS (U.S. Soil Conservation Service, 1964) on a large number of North American catchments, or calibrated. In the case of spatially varying soil parameters, a modified maximum potential infiltration for each sub-catchment is computed as $S_i^* = c_s \cdot S_i$, with c_s adjusted through calibration and assumed constant within each macro-area.



[Routing to macro-area node is performed using GIUH]
 [Baseflow is transferred to macro-area node using a linear bucket model]

Figure 2: Sketch of the hydrological processes simulated by GEOTRANSF at the sub-catchment scale.

Rainfall excess r_s is then routed to the river network as surface runoff, while infiltration constitutes the input term of the first of two nonlinear buckets connected in series, which mimic soil water dynamics within the hillslopes and sub-surface contribution to streamflow (Fig. 2).

The first bucket represents the rhizosphere, the upper layer of soil where infiltration, evapotranspiration and leakage to the underlying bucket are the active hydrological fluxes. The leakage flux from both buckets connected in series is computed as follows (Rodríguez-Iturbe and Rinaldo, 1997, ch. 2.1.6):

$$q_j(t) = \begin{cases} \beta_j \left[\exp \left\{ \frac{[\theta_j(t) - \theta_{0,j}] b_j}{m_j} \right\} - 1 \right] & \text{if } \theta_j(t) > \theta_{0,j} \\ 0 & \text{if } \theta_j(t) \leq \theta_{0,j} \end{cases} \quad (4)$$

where q_j [L/T], is the specific flux generated by the first ($j = 1$) or the second ($j = 2$) bucket, representing the upper and the lower soil layers, respectively. In addition, β_j [L/T] is a parameter controlling the maximum specific flux (i.e., the water flux per unitary contributing area) from the buckets, $\theta_{0,j}$ [-] is a soil water threshold below which water flux stops, b_j is the soil thickness and m_j [L] is a parameter controlling the rate of flow variation with soil water content.

The leakage from the second bucket is divided into two components by means of the partition coefficient c_p . The fraction $(1 - c_p) q_2$ contributes to streamflow, while the remaining fraction $c_p q_2$ feeds the deep underground storage. This two-bucket soil model is applied separately to each of the sub-catchments comprising the macro-area, with parameters that can be either constant for all the sub-catchments, or spatially variable.

Two conceptual models can be used for the baseflow. In the first conceptual model baseflow is accounted for directly through Eq. (4), such that the fraction of the leakage from the second bucket, $c_p q_2$, is lost in the deep bucket and does not enter the river network. In the second conceptual model, deep storage is modeled as a linear bucket with mean residence time k_{us} (Fig. 2).

The baseflow $q_b(t)$ is then obtained by solving the following mass balance equation:

$$v(t) = v(t - \Delta t) + \frac{c_p}{A_t} \sum_{i=1}^N q_{2,i}(t - \Delta t) A_i \Delta t - q_b(t - \Delta t) \Delta t \quad (5)$$

where v [L] is the specific storage in the macro-area deep bucket, which is related to the baseflow through the following relationship: $q_b(t) = v(t)/k_{us}$, and $q_{2,i}$ is the leakage flux from the second soil bucket. The baseflow generated by the macro-area is directly transferred to the control section without further delay or transfer functions.

The soil water content θ_j , $j = 1, 2$ in the two nonlinear buckets is obtained by applying the following two mass balance equations to each sub-catchment of the macro-area (see Fig. 2):

$$\theta_1(t) b_1 = \theta_1(t - \Delta t) b_1 + h_{eff}(t) - q_1(t - \Delta t) \Delta t - ET_{real}(t) \Delta t + \Delta U_1 \quad (6)$$

and

$$\theta_2(t) b_2 = \theta_2(t - \Delta t) b_2 + q_1(t - \Delta t) \Delta t - q_2(t - \Delta t) \Delta t - \Delta U_2 \quad (7)$$

In Eqs. (6) and (7) ΔU_1 [L] and ΔU_2 [L] are the specific volumes associated to water uses within the sub-catchment, which are positive in case of injection and negative in case of abstraction. Typical water uses that can be modeled with this scheme are irrigation in the first layer ($\Delta U_1 > 0$) and abstraction by water wells in the second layer ($\Delta U_2 < 0$). Notice that the volume of water extracted from bucket 2 can be injected as irrigation in bucket 1 of the same, or different, sub-catchment, thereby providing a full coupling between hydrological processes and water tapped from groundwater wells.

3.2. Routing along the river network

This module is designed for propagating (routing) downstream to the control section the water fluxes produced by sub-catchments and computed as described in Section 3.1, taking into account also water transfers related to water uses, as will be discussed in Section 4.

Routing is performed by using the Geomorphological Instantaneous Unit Hydrograph (GIUH) approach (Rodriguez-Iturbe and Valdes, 1979; Rodriguez-Iturbe and Rinaldo, 1997), as follows:

$$Q_{s,j} = \int_0^t Q_{in,j}(\tau) f_{s,j}(t - \tau) d\tau \quad (8)$$

where

$$Q_{in,j} = A_j \left[r_{s,j}(t) + q_{2,j} + q_{d,j}^* \right] \quad (9)$$

is the water discharge produced by the j -th sub-catchment modified by the water discharge $A_j q_{d,j}^*$, which represents the net effect of water uses within the sub-catchment, with the convention that withdrawal fluxes are negative, while restitution fluxes are positive (restitution fluxes includes also those originating outside the catchment and eventually those coming from sub-surface wells). In addition, $f_{s,j}$ is the transfer function of the sequence of the n_j stream elements connecting the sub-catchment j to the control section:

$$f_{s,j} = f_{j,(1)} * f_{j,(2)} * f_{j,(3)} * \dots * f_{j,(i)} * \dots * f_{j,(n_j)} \quad (10)$$

where the symbol $*$ indicates the convolution and $f_{j,(k)}$, with $k = 1, \dots, n_j$, is the transfer function of the k -th stream element in the ordered sequence of n_j streams connected in series.

According to the GIUH theory the transfer function of the stream element coincides with the pdf of residence time, which can be approximated by the following exponential relationship:

$$f_i(t) = \frac{1}{K_i} \exp\left[-\frac{t}{K_i}\right], \quad i = 1, \dots, N \quad (11)$$

where K_i is the mean residence time of the stream i , which is given by the ratio between the stream length L_i and the average velocity $v_{s,i}$. The latter is estimated by the following geomorphological relationship:

$$v_{s,i} = c \left(A_c^i \right)^\gamma, \quad (12)$$

where $A_c^i [L^2]$ is the total cumulated area, defined as the sum of the contributing areas of all the sub-catchments draining directly, or indirectly, into the stream i , and c is a proportionality coefficient. This formulation, in which the total cumulated area is a proxy of average stream velocity, is supported by several geomorphological studies, starting from the seminal work by Leopold and Maddock (1953) and recently reviewed by Dodov and Fofoula-Georgiou (2004a). In order to limit the number of parameters the exponent γ in (12) has been fixed equal to 0.15, which represents an intermediate value of the experimental range 0.1 – 0.3 observed in literature (see e.g., Dodov and Fofoula-Georgiou, 2004b; Orlandini, 2002). A detailed analysis of the uncertainty associated to the estimation of this exponent has been recently proposed by Orlandini (2002) and Orlandini et al. (2006) with reference to steep Alpine streams, which investigation is however beyond the scope of the present work. The only unknown is thus the proportionality coefficient c , which will be obtained by calibration for each macro-area of the river basin.

The convolution of n_j exponential pdfs assumes the following general form (Rodriguez-Iturbe and Valdes, 1979):

$$f_{s,j} = \sum_{i=1}^{n_j} C_{i,n_j} e^{-t/K_{j(i)}}, \quad C_{i,n_j} = K_{j(i)}^2 \prod_{l=1, l \neq i}^{n_j} [K_{j(i)} - K_{j(l)}]^{-1} \quad (13)$$

where $K_{j(i)}$ is the mean residence time in the i -th stream in the sequence of n_j ordered streams, with the number within brackets that identifies the stream occupying the i -th position in the sequence (notice that the same stream can assume different positions along ordered stream sequences depending on the sub-catchment from which the sequence originates). When all the streams share the same mean residence time K , Eq. (13) reduced to the Gamma pdf (Feller, 1971):

$$f_{s,j} = \frac{1}{t \Gamma(n_j)} \left(\frac{t}{K} \right)^{n_j} e^{-t/K} \quad (14)$$

where n_j , and $1/K$ are the shape and rate parameters, respectively, and $\Gamma(n_j) = \int_0^\infty r^{n_j} e^{-r} dr$ is the complete Gamma function. The sequential convolution of exponential transfer functions is therefore equivalent to adopt a generalized form of the Gamma function with the mean residence time depending of the total cumulated area, which has been shown a good descriptor of the recession limb of streamflow following an impulse trigger by rainfall in a wide range of geomorphic conditions (Labat et al., 2000; Kirchner et al., 2001; Majone et al., 2004, 2010; Botter et al., 2013). More sophisticated geomorphological relationships for the estimation of stream velocity, as well as non-linear routing methods (e.g. Muskingum-Cunge) can be easily implemented in case of need.

4. Human system

The human system is represented as diversion channels connected to the streams either directly or by means of reservoirs. Each diversion channel can end in another node of the river network or within sub-catchments. Water budgets, which determine the modification of the natural hydrological fluxes due to water uses, are performed at the nodes of the network where the human system is connected through the confluence module. This module allows also to sum contributions from other macro-areas, aquifers, or hydraulic infrastructures, connected to the node. The water budget is performed under physical and regulatory constraints, such as, for example, the maximum capacity of the withdrawal channel, or the intake works, and the obligations to respect the minimum ecological flow and protocols regulating the interactions with downstream uses.

4.1. Water use element

Water transfers within and outside the river basin are grouped into two categories: i) large water transfer systems, including storage reservoirs if present, and ii) all the other small withdrawals (i.e., agricultural, civil, and industrial water uses and small run-of-the-river power plants). Notice that the separation between large and small water uses is decided by the user and this choice affects the number of nodes where water budget is performed and water discharge is computed.

Large hydraulic systems, such as large hydropower and water transfer systems with reservoirs, are treated separately, because the assessment of their impact on streamflow requires detailed information on both hydraulic structures

and management rules. In addition, the introduction of a reservoir and the connection points between the river network and the intake/restitution channels requires the definition of new nodes in the network structure (see Fig. 1). This procedure ensures accuracy in describing water transfers, but add complexity to the river network and therefore cannot be applied to small licensed uses, which are typically very large in number and distributed through the catchment. Conversely, one of the main features of GEOTRANSF is the inclusion of these utilizations aggregated at the sub-catchment scale, while respecting the constraints resulting from their hierarchical distribution along the unmodeled (sub-grid) river network.

Each small licensed use is characterized by a withdrawal and a release (restitution) point with the exception of sub-surface withdrawals and irrigation releases, which are first cumulated at the sub-catchment scale and then introduced into the soil water budgets (6) and (7) (see Fig. 2). Point water withdrawals and releases located within the sub-catchment, are accounted for hierarchically. The sequence in which the licensed withdrawals or restitutions are considered can either be set during DTM pre-processing (see Sect. 5), or set manually by the user. The effect of water diversion (restitution) at a specific location within the sub-catchment k is evaluated by assuming that the amount of water available in the stream is a fraction of the streamflow $Q_{in,k}$ generated within the sub-catchment (only the natural component is considered here) reduced (augmented) by the water discharge withdrawn (released) upstream. Therefore, the available streamflow $Q_{i,k}^a$ at a given licensed location i within the sub-catchment k , where inflow (release) or outflow (withdrawal) occurs, can be calculated as follows:

$$\begin{aligned} Q_{i,k}^a &= \alpha_{i,k} Q_{in,k} + Q_{i,k}^* && \text{(secondary streams)} \\ Q_{i,k}^a &= Q_{str,k} + \alpha_{i,k} Q_{in,k} + Q_{i,k}^* && \text{(main stream)} \end{aligned} \quad (15)$$

where $Q_{str,k}$ is the streamflow entering the sub-catchment from outside through the mainstream, $Q_{i,k}^* = \sum_{j=1}^{i-1} Q_j^d$ is the sum of the external fluxes released (positive) or withdrawn (negative), already taken into account because lower in the hierarchy order (within the sub-catchment) and $\alpha_{i,k} = A_{i,k}/A_k$ is the ratio between the contributing area $A_{i,k}$ at the same node and the sub-catchment area A_k . An explanatory example of how this is performed is presented in Fig. 3 for the case of four withdrawals without restitution. Notice that the term $Q_{i,k}^*$ may represent water transfers between points not necessarily located within the same sub-catchment, and that $Q_{str,k} = 0$ for headwater sub-catchments feeding first-order (in the Strahler classification) streams. Therefore, the flux $q_{d,j}^*$ to be included into Eq. (9) is given by: $q_{d,j}^* = Q_{nd_j}^*/A_j$, where nd_j is the number of small license locations within the sub-catchment. Moreover, all water diversions are simulated by taking into account the constraints introduced by both MEF and the maximum water discharge that intakes allow to be withdrawn.

4.2. Reservoir element

The effect of a reservoir is evaluated by solving the following water budget equation:

$$\frac{dV(h)}{dt} = Q_{r,in}(t) - Q_{r,spill}(t, h) - Q_{r,mef}(t) - Q_w(t) \quad (16)$$

where $Q_{r,in}$ is the reservoir inflow evaluated at the node of the network representing the reservoir, $Q_{r,spill}$ is the outflow from flood gates, $Q_{r,mef}$ is the MEF release, and $Q_w(t)$ is the water discharge withdrawn from the reservoir through the intake. Notice that $Q_{r,spill}$ depends both on time and the water elevation h in the reservoir, since flood gates can be operated or held fixed, depending on the operational rules and that in case of hydropower use with powerhouse at the toe of the reservoir Q_w is aggregated to $Q_{r,mef}$. In addition, $V(h)$ is the volume stored within the reservoir when it is at the elevation h . Furthermore, Eq. (16) assumes implicitly that losses due to evaporation from the reservoir surface are balanced by direct precipitation and undetected sub-surface fluxes. However, more general situations with the inclusion of these components can be easily envisioned with small modifications of the budget expressed by Eq. (16). In the current implementation of the model, target values of Q_w are assigned either on the basis of observed historical data or according to reservoir-specific management rules, which include priorities (e.g., MEF releases) and limitations for flood protection. Eq. (16) is resolved with an explicit finite difference method given the water level at the starting time of the simulation.

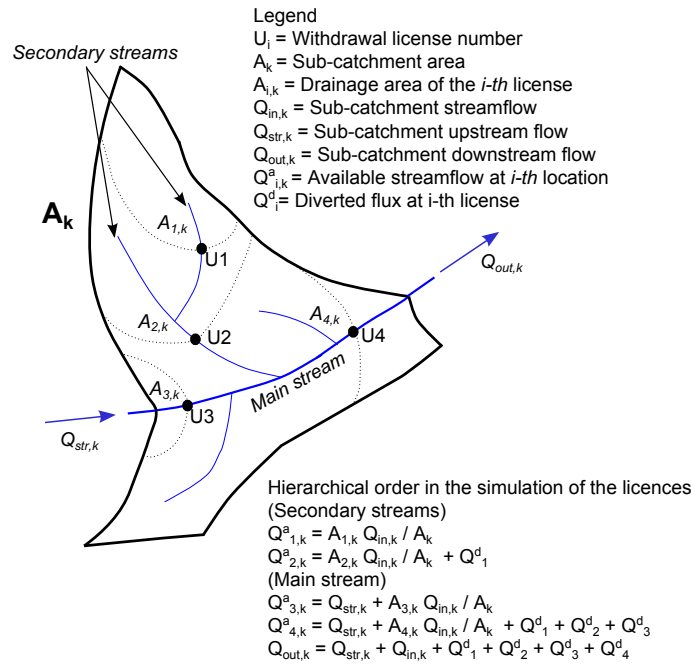


Figure 3: Synthetic example of the hierarchical order adopted for the simulations of 4 small licensed uses diverting water (negative flux) from a single sub-catchment of area A_k .

5. Data requirements

GEOTRANSF is designed to work with minimal meteorological information consisting of precipitation and temperature data. However, observed streamflow data are needed when applying inverse modeling to infer model parameters from observational data. River network topology is extracted from a DTM and maps of soil type and land use are consulted to assign spatially variable parameters to the SCS-CN model of infiltration.

The model is provided with a proprietary GUI named AWDT-GeometryBuilder (developed and maintained by Smart Hydrogeological Solutions S.r.l.), designed to identify the river network and the associated sub-catchments and compute their attributes for successive use in the modeling activities. AWDT-GeometryBuilder performs also DTM pre-processing operations such as, depitting (by using a modified version of the Planchon-Darboux approach, 2001, for flat areas removal) and reconditioning (following a methodology similar to "AgreeDem" implemented in HecGEOhms package developed by the U.S. Army Corps). However, other GIS environments can be adopted for watershed analysis.

Including anthropogenic impacts in the model requires additional information on the functioning of large hydraulic infrastructures, such as reservoirs and diversion channels, and of small withdrawals (i.e. small hydropower plants, agricultural, civil and industrial uses, fish farming etc.) as well. As already discussed in Sect. 4.1 these two types of water uses are considered separately mainly because typically the latter outnumbers the former, thereby calling for a different strategy of data collection and implementation. Simulation of large hydraulic infrastructures requires several specific data, such as elevation-volume curves of the reservoirs, their maximum and minimum regulation levels and possibly time series of water level, inflow and outflow water discharges during an extended period of observation. Locations and maximum withdrawal capacities of the diversion channels connected to the reservoirs are also needed in order to properly represent water transfer within the river basin, and in some cases also transfers between conterminous catchments. For small licensed uses, information regarding the location of withdrawal and restitution points is needed in addition to the typology of the withdrawal and the maximum allowed water fluxes. Furthermore, in order to take into account environmental issues related to water withdrawals, GEOTRANSF applies to each individual location the MEF release as imposed by the specific regulatory protocol.

6. Inverse modeling and parameter identification

Model's parameters can be obtained either by using a classical calibration procedure, aimed at identifying a single optimal, in some sense, set of parameters, or within a Bayesian framework by computing the a posteriori probability distribution of the parameters (see e.g., Vrugt et al., 2003; Liu and Gupta, 2007; Rubin et al., 2010). In the present version of the software searching of the parameters space is performed by using the Particle Swarm Optimization (PSO) technique (Robinson and Rahmat-Samii, 2004; Castagna and Bellin, 2009; Majone et al., 2010), with the Nash-Sutcliffe efficiency coefficient as objective function:

$$NS = 1 - \frac{\sigma_e^2}{\sigma_o^2} \quad (17)$$

where σ_o^2 is the variance of the observed streamflow signal and σ_e^2 is the variance of the residuals, which are defined as the difference between observed and computed streamflow. PSO is a robust stochastic evolutionary optimization technique based on the movement of a swarm of bees. The application of this algorithm is particularly suited to calibration procedures in the presence of large number of parameters since it is insensitive to both initial conditions and the shape of the efficiency function.

Inversion estimates the value of parameters that are characteristic of the area contributing to the control section where streamflow is measured, which is the total contributing area reduced by the area contributing to the upstream control sections where inversion is also performed (see Fig. 1c). Therefore, inversion (calibration) starts at the most upstream control sections and proceeds hierarchically with the other nodes after removing from the contributing area the portions of the catchment contributing to the upstream nodes. The water discharge at the upstream control sections is transferred to the selected control section by convolution with the transfer function (10) applied to the sequence of streams connecting the two nodes. In doing that, different sets of parameters are attributed to each portion of the catchment contributing to the selected control sections. Water volumes transferred outside the area contributing to the control section are included as external fluxes to other control sections. In case of poor performance (i.e., small Nash-Sutcliffe parameter values) of the inversion, the node at which this happens can be excluded to avoid propagation of the error downstream and the corresponding macro-area is cumulated to the closest downstream node. This is a pragmatic choice of this version of the software. However multi-site calibration techniques may be employed as suggested by Cao et al. (2006); Nalbantis et al. (2011); Ahmadi et al. (2014), without changing the hydrological modules.

The list of model parameters is reported in Table 1. They can be set to given values in a forward modeling approach, or to initial values for the parameters space searching through PSO. As discussed above a set of parameters is identified for each macro-area (i.e., control section).

7. Examples of application

GEOTRANSF has been successfully applied to evaluate the projected impact of climate change on streamflow and water resources in the Gállego catchment, Spain (Majone et al., 2012). In the same catchment it has also been coupled with an agro-economic model to evaluate the combined effect of climate change and economic scenarios (Graveline et al., 2014). Furthermore, a number of studies have been conducted to assess the local impact of the water uses in the Province of Trento, the administrative unit responsible of the management of several catchments in the southeastern Alps.

To exemplify the application of the model and show the accuracy that can be achieved in modeling the hydrological cycle in a case of interest for applications, we discuss here the case of the Noce catchment, a medium size Alpine catchment with a strong elevation gradient and relevant water uses, mainly for hydropower.

7.1. Noce river basin

The Noce river is located in the Southeastern Alps, Italy, and is one of the main tributaries of the Adige River. At the confluence with the Adige river its length is of 82 km, its total contributing area is 1,367 km² and the average slope of the catchment is 3.04% (see Fig. 4). Headwaters in the upper part of the catchment show a typical Alpine glacial regime. Presena and Presenella glaciers, located in the southern portion of the catchment and belonging to the Adamello-Presanella system, one of the most important glacial systems of the southern Alps, feed the Vermigliana

Table 1: List of model parameters.

| Description | Symbol | Model Component |
|--|------------------------|--------------------|
| sub-surface flow variation rate (layer 1) | $m_1[L]$ | sub-surface flow |
| sub-surface flow variation rate (layer 2) | $m_2[L]$ | sub-surface flow |
| sub-surface flow partition coefficient (layer 2) | $c_p[-]$ | sub-surface flow |
| soil depth (layer 1) | $b_1[L]$ | sub-surface flow |
| soil depth (layer 2) | $b_2[L]$ | sub-surface flow |
| residual water content (layer 1) | $\theta_{0,1}[-]$ | sub-surface flow |
| residual water content (layer 2) | $\theta_{0,2}[-]$ | sub-surface flow |
| maximum specific water flux (layer 1) | $\beta_1[L/T]$ | sub-surface flow |
| maximum specific water flux (layer 2) | $\beta_2[L/T]$ | sub-surface flow |
| field capacity | $\theta_{fc}[-]$ | evapotranspiration |
| residual water content | $\theta_r[-]$ | evapotranspiration |
| multiplicative coefficient for threshold parameter triggering runoff | $c_a[-]$ | rainfall excess |
| multiplicative coefficient for maximum infiltration capacity | $c_s[-]$ | rainfall excess |
| threshold air temperature below which precipitation is always solid, | $T_s[^\circ C]$ | snow |
| threshold air temperature above which melting occurs | $T_{sm}[^\circ C]$ | snow |
| melting factor | $c_{melt}[L/^\circ C]$ | snow |
| linear bucket constant | $k_{us}[T]$ | baseflow |
| parameter controlling streamflow velocity | $c[L^{-0.3}L/T]$ | GIUH routing |

creek, while the Noce Bianco receives the contribution of the Careser glacier, which is part of the Ortles-Cevedale system and faces from North the other two glaciers. Noce di Valle del Monte joins the Noce Bianco at Cogolo and downstream this confluence the river is named Noce. Moving further downstream it receives first the contribution of the Vermigliana and successively, after receiving the contribution of other minor tributaries, it shifts its regime from glacial to mixed glacial and nival. The characteristics of the streamflow and the identification of the main contributions of the Vermigliana creek, which shows a typical glacial regime, are discussed in the work by Chiogna et al. (2014), while stress factors for the freshwater ecosystem are discussed in Chiogna et al. (2015), to which we refer for further details.

Table 2: Main characteristics of reservoirs and power plants within the Noce river basin.

| Reservoir | Careser | Malga Mare | Pian Palù | Santa Giustina | Mollaro |
|---------------------------------------|------------|------------|-----------|----------------|-------------|
| Hydropower Plant | Malga Mare | Cogolo 1 | Cogolo 2 | Taio | Mezzocorona |
| Max. Storage [$10^6 m^3$] | 15.580 | 0.033 | 15.510 | 186.294 | 0.864 |
| Min. Regulation Volume [$10^6 m^3$] | 0.333 | 0.000 | 0.244 | 11.140 | 0.000 |
| Max. Regulation Volume [$10^6 m^3$] | 15.580 | 0.033 | 15.510 | 182.810 | 0.864 |
| Available Volume [$10^6 m^3$] | 15.247 | 0.033 | 15.266 | 171.670 | 0.864 |
| Max. Water Flow [m^3/s] | 3.000 | 6.400 | 7.600 | 66.000 | 60.000 |

Timber forest covers the majority of the catchment area (56.5%), followed by bare rocks (16.4%), pasture land (15.4%) and agriculture fields (6.2%). Urban areas, distributed in small villages along the valleys bottom, occupies 2.8% of the territory, while the remaining of the area (2.7%) is occupied by water bodies and glaciers. From a geological point of view paragneiss dominates the northern part of the catchment, which are replaced by ortogneiss, micaschists and phyllite in the central part. Tonalite and carbonate rocks characterize the eastern and southern portions of the catchment, where karst phenomena have been also observed. Climate is cold and wet with a mean annual temperature of $3.9^\circ C$ and mean annual precipitation of 1170 mm/year, with significant snowfalls in winter.

Water uses within the catchment are dominated by five large hydropower plants (Majone et al., 2015): Malga Mare, Cogolo1 and Cogolo2 in the upper catchment, operated by Dolomiti Energia Spa, and Taio and Mezzocorona, in the middle to lower course of the river, both operated by Edison-HDE Spa. Hydropower production of these power plants is regulated with 5 reservoirs: Pian Palù, Careser, Malga Mare, which are part of the system composed of three power plants in the upper catchment, Santa Giustina and Mollaro, feeding the Taio and Mezzocorona power plants, respectively, in the middle to lower catchment (see Fig. 4). These reservoirs provide a total storage capacity

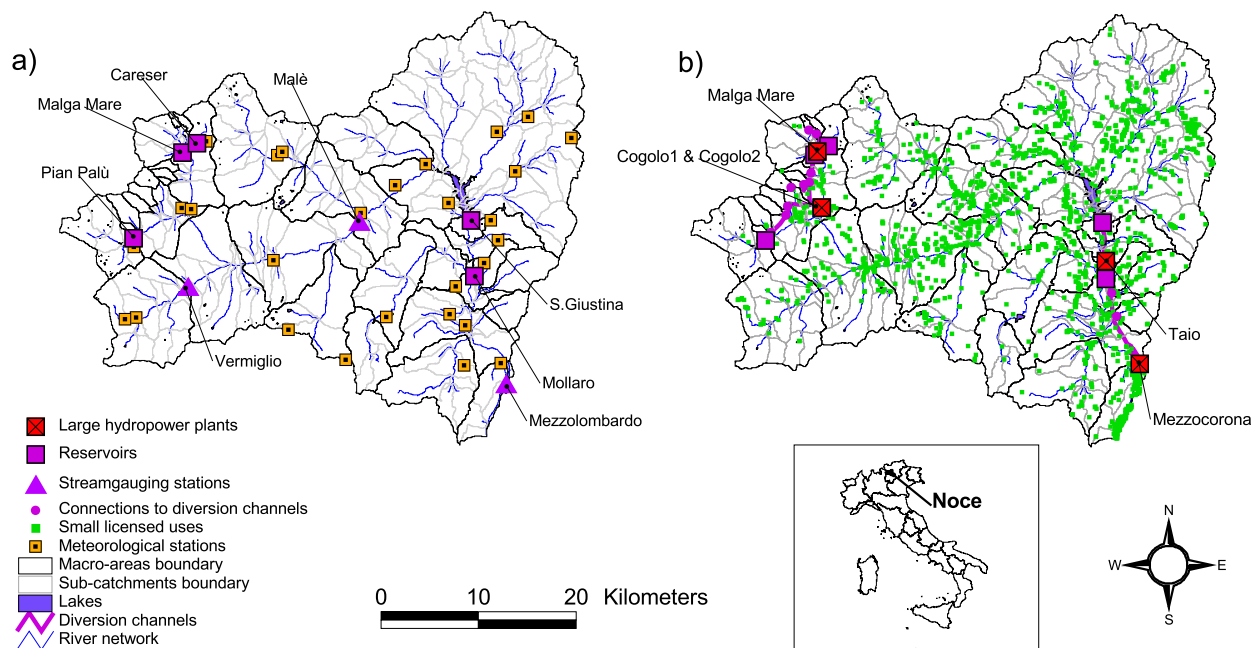


Figure 4: Map of the Noce river basin with indicated: a) the partition in macro-areas (black continuous lines) and sub-catchments (gray continuous lines in the background), location of streamflow gauging stations, reservoirs and meteorological stations; and b) channel network connecting the main hydropower systems in the area, i.e. hydropower with average nominal capacity larger than 3 MW, and intake works. Green bullets indicate small licensed uses. The inset shows the geographic location of the Noce river basin within the Italian territory.

of $203 \times 10^6 m^3$. The main characteristics of the reservoirs are reported in Table 2, whilst the locations of the power plants and of the diversion channels are depicted in Fig. 4b. Reservoirs are managed according to the rules described in specific protocols included in the Water Uses General Plan (PGUAP, 2006) of the Province of Trento (available online at <http://pguap.provincia.tn.it>), which, for example, defines the MEF releases to maintain the ecological functionality of the rivers. Rules for combined agricultural and hydropower uses are included in specific protocols and are under discussion. Furthermore, flood risk is managed by allocating permanent extra storage capacity to the reservoirs with the possibility of preventive releases from the main reservoirs to create additional extra free volumes for storing incoming floods. Releases are regulated by specific protocols and are ordered by the flood control authority (flood control bureau of the Provincia Autonoma di Trento).

The Malga Mare power plant uses the water stored in the Careser reservoir, which collects the streamflow originating from the Careser glacier and a small catchment between the tongue of the glacier and the reservoir. The power plant is designed to use up to $3.0 m^3/s$. The water exploited by the Malga Mare power plant is discharged into a small impoundment of $0.033 \times 10^6 m^3$ (see Table 2), bearing the same name, which receives also the contribution of the "La Mare" glacier. Water stored in the reservoir is used in the Cogolo power plant, which receives also the contribution arriving from the Pian Palù reservoir. The maximum water discharge from the Malga Mare reservoir is of $6.4 m^3/s$ and is used in a group of 2 turbines named Cogolo1, while the maximum water discharge from the Pian Palù is $7.6 m^3/s$ distributed to another group of 2 turbines named Cogolo2. In the middle course of the river streamflow, including that exploited by the above power plants, is stored into the reservoir of Santa Giustina, to be used in the Taio power plant. The maximum water discharge that this power plant can use is $66 m^3/s$. The water discharge exploited by the Taio power plant, together with that released from the Santa Giustina reservoir as MEF, is subsequently stored within the Mollaro reservoir and transferred to the Mezzocorona power plant, which may use up to $60 m^3/s$.

In addition to the above large hydroelectric power plants, water resources of the catchment are intensively exploited with a large number of small water uses (1974 withdrawals for a total licensed annual volume of $1.3 \times 10^9 m^3$) composed of 100 small run-of-the-river power plants (i.e., with average nominal capacity smaller than 3 MW) installed chiefly in head waters and diffuse withdrawals for agricultural (for irrigation and fish farming), civil and industrial

uses (see Table 3). Other activities such as sport fishing, rafting and canoeing, which are important for the touristic sector in the upper valley, impose additional limitations (La Jeunesse et al., 2015), with the last two requiring water levels above a given threshold in selected river reaches in late spring and summer.

7.2. Model Setup

Table 3: Total annual licensed volumes and number of withdrawals other than large hydropower (average nominal capacity larger than 3 MW), classified according to categories.

| Water use | Total Annual Volume [$10^6 m^3$] | Number of licenses |
|-------------------------|---------------------------------------|--------------------|
| Agricultural | 148.17 | 876 |
| Civil | 56.99 | 888 |
| Industrial | 6.43 | 47 |
| Small Hydropower Plants | 897.58 | 100 |
| Others | 18.95 | 63 |
| Total | 1128.15 | 1974 |

Simulations were conducted for the period 2000-2006 with a daily time step by using continuous time series of water discharge at the gauging stations of Vermiglio, Malè and Mezzolombardo (see Fig. 4a), supplemented by the time series of inflow at 4 out of 5 reservoirs (the data of Mollaro reservoir were excluded because unreliable), as observational data. In addition water level data were available at the 5 reservoirs. In order to minimize the effects of the initial conditions on the inference of the model's parameters, the year 2000 is simulated but not included into the objective function. The meteorological forcing is described with daily precipitation and temperature at 28 meteorological stations provided by MeteoTrentino (<http://www.meteotrentino.it>) and Edmund Mach Foundation (<http://meteo.fmach.it/meteo/dati.php>) both running an independent network of meteorological stations. Fig. 4a shows a map with the locations of the meteorological stations.

In the present study each sub-catchment was assigned with a value of the maximum potential infiltration (S) and the crop coefficient K_c , both obtained as weighted average of the values estimates at each DTM cell by using the available infiltration capacity and soil use maps provided by the Autonomous Province of Trento (available online at <http://pguap.provincia.tn.it>).

The model contains a detailed description of reservoir and power plants functioning with an accurate identification of the points where water is withdrawn and/or restituted to the river, as discussed in Sect. 4. The catchment is divided into 228 channels and sub-catchments (each channel receives the contribution of a sub-catchment), with a mean contributing area of $5.9 km^2$. The sub-catchments are aggregated into 36 macro-areas, according to the spatial distribution of water withdrawals and restitution shown in Figs. 4a and 4b. The control sections adopted for the calibration and validation procedure are located at 4 out of 5 reservoirs considered in the study (Pian Palù, Careser, Malga Mare and Santa Giustina) and at 3 stream-gauge stations (Vermiglio, Malè and Mezzolombardo, with the latter being the outlet of the river basin). Consequently, 7 macro-areas with a different set of parameters are identified

To reduce the number of calibration parameters the following assumptions have been introduced, as suggested by a preliminary sensitivity analysis: i) the soil depth of the first layer b_1 is fixed to 1000 mm, which is a reasonable average thickness of the rhizosphere, ii) soil water thresholds $\theta_{0,j}$ and residual water content θ_r are fixed to 0.05 and 0.0, respectively, on the basis of previous hydrological studies conducted with GEOTRANSF (Majone et al., 2012, 2015), iii) the following assumption: $\beta_1 = \beta_2 = \beta$ is employed, and iv) the soil parameters m_1 and m_2 satisfy the following relationship: $m_2 = m_1 * b_2/b_1$. This latter assumption is equivalent to considering a constant equivalent hydraulic conductivity for the two strata, with the parameter m being related to the equivalent saturated hydraulic conductivity of the sub-catchment as shown in Majone et al. (2010). Furthermore, sensitivity analysis showed that including the baseflow from the groundwater storage does not lead to a significant improvement in the model performance. This is due to the lack of independent information on groundwater dynamics which does not allow a firm separation of relatively fast sub-surface flow, from slow groundwater flow (Piccolroaz et al., 2015). Therefore, given the poor identifiability of the storage parameters, the groundwater component of the water budget has been excluded. In addition, the adopted simulation time step (i.e., 1 day) resulted larger than the residence time of water in the river network and thus flow routing has been neglected in the streamflow generation process. These two simplifications in

the conceptual model are suggested by the particular case at hand and can be removed when suggested by observational evidences.

7.3. Calibration and validation

Table 4: Estimated model parameters and *NS* index during calibration and validation periods for the 7 control sections within the catchment. Parameters assigned to a constant value and not calibrated are marked with an asterisk.

| | Pian Palù | Careser | Malga Mare | Vermiglio | Malè | Santa Giustina | Mezzolombardo |
|----------------------------|-------------|-------------|-------------|-------------|-------------|----------------|---------------|
| m_1 [mm] | 25.37 | 22.53 | 34.18 | 10.03 | 20.75 | 24.80 | 24.68 |
| $m_2 = m_1 * b_2/b_1$ | - | - | - | - | - | - | - |
| c_p [-] | 0.20 | 0.15 | 0.08 | 0.13 | 0.60 | 0.11 | 0.00 |
| b_1^* [mm] | 1000.0 | 1000.0 | 1000.0 | 1000.0 | 1000.0 | 1000.0 | 1000.0 |
| b_2 [mm] | 3040.2 | 2281.3 | 1293.6 | 2851.2 | 2273.8 | 5933.5 | 9960.1 |
| $\theta_{0,1}^*$ [-] | 0.05 | 0.05 | 0.05 | 0.05 | 0.05 | 0.05 | 0.05 |
| $\theta_{0,2}^*$ [-] | 0.05 | 0.05 | 0.05 | 0.05 | 0.05 | 0.05 | 0.05 |
| β_1 [$m^3/s/km^2$] | $1.0E^{-2}$ | $1.1E^{-2}$ | $1.0E^{-2}$ | $1.3E^{-2}$ | $1.1E^{-2}$ | $1.3E^{-4}$ | $7.4E^{-3}$ |
| $\beta_2 = \beta_1$ | - | - | - | - | - | - | - |
| θ_{fc} [-] | 0.40 | 0.40 | 0.16 | 0.40 | 0.15 | 0.16 | 0.39 |
| θ_r^* [-] | 0.00 | 0.00 | 0.00 | 0.00 | 0.00 | 0.00 | 0.00 |
| c_a [-] | 0.10 | 1.00 | 0.36 | 0.12 | 0.11 | 0.10 | 0.10 |
| c_s [-] | 5.03 | 1.22 | 2.33 | 4.01 | 2.58 | 5.88 | 2.87 |
| T_s [$^{\circ}C$] | -0.99 | -1.63 | -1.68 | 0.46 | 0.49 | 0.48 | 0.30 |
| T_{sm} [$^{\circ}C$] | 0.51 | 1.92 | 0.51 | 1.35 | 0.61 | 3.29 | 1.78 |
| c_m [mm/ $^{\circ}C/d$] | 2.73 | 2.58 | 3.16 | 2.49 | 1.91 | 6.44 | 3.60 |
| k_{us} [h] | - | - | - | - | - | - | - |
| c ($km^{-0.3}m/s$) | - | - | - | - | - | - | - |
| <i>NS cal</i> | 0.87 | 0.80 | 0.82 | 0.83 | 0.95 | 0.88 | 0.94 |
| <i>NS val</i> | 0.76 | 0.63 | 0.76 | 0.73 | 0.90 | 0.73 | 0.96 |

Table 5: Average monthly and annual observed and simulated streamflow (m^3/s) for the 7 control sections within the catchment in the period 2001-2006.

| | Pian Palù | | Careser | | Malga Mare | | Vermiglio | | Malè | | Santa Giustina | | Mezzolombardo | |
|-----------|-----------|------|---------|------|------------|------|-----------|------|-------|-------|----------------|-------|---------------|-------|
| | Obs | Sim | Obs | Sim | Obs | Sim | Obs | Sim | Obs | Sim | Obs | Sim | Obs | Sim |
| January | 0.44 | 0.40 | 0.13 | 0.10 | 0.82 | 0.89 | 0.82 | 0.58 | 5.21 | 4.87 | 14.97 | 16.73 | 35.88 | 32.66 |
| February | 0.38 | 0.36 | 0.13 | 0.09 | 1.01 | 1.14 | 0.66 | 0.41 | 4.85 | 4.90 | 14.19 | 14.38 | 39.46 | 35.69 |
| March | 0.43 | 0.38 | 0.15 | 0.08 | 1.26 | 1.36 | 0.86 | 0.51 | 5.88 | 6.03 | 15.13 | 15.93 | 34.19 | 29.51 |
| April | 0.67 | 0.56 | 0.17 | 0.08 | 1.02 | 1.03 | 1.58 | 1.02 | 7.18 | 7.62 | 17.01 | 16.83 | 24.88 | 20.41 |
| May | 3.13 | 3.15 | 0.66 | 0.50 | 1.91 | 1.51 | 6.61 | 5.95 | 20.85 | 20.93 | 40.54 | 38.61 | 36.86 | 31.83 |
| June | 5.24 | 5.32 | 2.20 | 1.99 | 3.78 | 2.93 | 7.82 | 7.25 | 24.03 | 24.87 | 42.58 | 41.85 | 48.38 | 46.21 |
| July | 3.67 | 3.66 | 2.29 | 2.27 | 4.42 | 3.98 | 6.00 | 5.82 | 19.50 | 21.46 | 33.70 | 34.09 | 44.15 | 43.78 |
| August | 2.40 | 2.22 | 1.61 | 1.45 | 3.37 | 3.22 | 4.08 | 4.09 | 12.49 | 14.52 | 21.98 | 24.26 | 28.87 | 29.43 |
| September | 1.57 | 0.19 | 0.82 | 0.03 | 2.26 | 0.24 | 2.28 | 0.88 | 9.31 | 1.68 | 18.78 | 0.63 | 32.72 | 1.15 |
| October | 1.23 | 1.75 | 0.35 | 0.70 | 1.42 | 1.92 | 1.85 | 2.90 | 8.46 | 9.97 | 18.22 | 20.04 | 30.11 | 30.95 |
| November | 0.99 | 1.53 | 0.21 | 0.50 | 1.28 | 1.70 | 1.89 | 2.74 | 10.01 | 11.60 | 24.45 | 26.91 | 37.98 | 37.35 |
| December | 0.57 | 0.77 | 0.14 | 0.20 | 0.94 | 1.11 | 0.99 | 1.09 | 6.04 | 6.37 | 15.21 | 19.76 | 26.77 | 24.78 |
| Annual | 1.73 | 1.69 | 0.74 | 0.66 | 1.96 | 1.75 | 2.95 | 2.77 | 11.15 | 11.24 | 23.06 | 22.50 | 35.02 | 30.31 |

Calibration was performed by maximizing independently the NS metrics computed with the streamflow data at the 7 selected control sections during the period 1 January 2001 - 31 December 2003, with the year 2000 used as spin-up. The following period (1 January 2004 - 31 December 2006) was used for validation. The optimal parameter values maximizing the NS metrics were identified by exploring the space of the parameters by means of the PSO algorithm. In this application we knew water releases and diversions from the reservoirs such that the inference of the

operational rules was not necessary. However, when this information is not available, or it is limited to the time series of reservoir levels, operational rules may be inferred together with the model parameters by using multi-objective inference, but keeping in mind that this can be an error prone procedure, depending on the configuration of the system and the amount of available data (see e.g., Traynham et al., 2011). It should be observed, however, that in the case of the hydropower reservoirs operational rules can be inferred from available production data, with some limitations due to the time aggregation at which they are available.

Table 4 shows the optimal set of parameter values obtained at the seven control sections used for calibration, which resulted in *NS* efficiency coefficients always larger than 0.80. When applied to the 2004-2006 validation period these sets of parameter values provided a good reproduction of the streamflows with *NS* values slightly smaller than those obtained during calibration (see Table 4). Monthly and yearly average streamflow at the 7 control sections are reported in Table 5 for the overall period 2001-2006. Relative deviations between mean annual simulated and observed streamflows are smaller than 6.2% at 4 out of 7 control sections (i.e., Pian Palù, Vermiglio, Malè and Santa Giustina), increase slightly to ~ 10% for Careser and Malga Mare and to ~ 13.5% for Mezzolombardo, thereby suggesting that the simulations are not affected by bias. Seasonality of streamflows, as described by the variation of the monthly means, is in general well reproduced by the model at all the control sections with limited differences between simulated and observed monthly means (see Table 5). Largest deviations are indeed observed at upstream control nodes with maximum differences mostly concentrated in October to December. Fig. 5 compares measured streamflows at the 7 control sections during the period 2000-2006 with the model simulations. The model correctly reproduces peak flows, the timing and shape of storm events and also the recession curves in the periods between two consecutive rainfall events. Details on time series comparisons for 2002 are shown in the inset of each panel.

Table 4 shows limited variability of the optimal parameters estimated by inverting separately the hydrological data at the control sections, and this is an indication of robustness of the model and identifiability of the parameters, although it is impossible to separate uncertainty from intrinsic heterogeneity of the catchment. In particular, estimated values of m_1 , which embeds all non-linearities in the transformation of precipitation to water flow produced by the soil mantle, are in the range between 20.7 mm and 34.2 mm with the only exception of Vermiglio, for which $m_1 = 10$ mm, as a consequence of a more impulsive response to the meteorological forcing. Estimated values of lower layer soil thickness b_2 are also consistent since they increase moving from higher (e.g. Pian Palù, Careser, Malga Mare, Vermiglio) to intermediate (Malè and Santa Giustina) and lower (Mezzolombardo) altitudes, in agreement with the general understanding that soil is typically thin or absent on narrow ridge crests, and accumulates in the valleys (see e.g., Arnett, 1971; Dietrich et al., 1995). On the other hand, significant differences are observed in the values of the partition coefficient c_p , which separate the fraction of flow that reaches the stream from that feeding the underlying aquifer. This may be indicative either of a large spatial variability of groundwater recharge or its low identifiability with the available streamflow data, and calls for including in catchment scale modeling information about groundwater dynamic in order to better represent this component of the hydrological cycle (Piccolroaz et al., 2015).

Since in applications it is rather common the situation in which only general rules of reservoir management are available, we repeated the simulations by keeping fixed the hydrological parameters and considering daily values of the outflows from the reservoirs equal to the monthly averages of the period 2000-2006. We also assumed shutoff of all hydropower plants during the weekends, when the price of energy is typically low, except in the periods in which the reservoir reaches the maximum operational level. Owing to their small volume, the reservoirs of Malga Mare and Mollaro are represented by assuming that the flow diverted from the reservoir to the connected hydropower plant is equal to the incoming flow, as suggested by Figs. 6a and 6b showing, for the period 2000-2006, the observed values of diverted versus inflow at Malga Mare and Mollaro reservoirs, respectively. The dispersion observed in Fig. 6b is due to the larger volume of the Mollaro reservoir with respect to Malga Mare, which permits a limited, yet appreciable, flow regulation. In both cases an upper cutoff equal to the maximum water discharge that the hydropower system can use is imposed.

The resulting streamflows at the gauging stations were in a good agreement with those computed by using the measured outflows (results not shown) with the time evolution of the water volume in the three main reservoirs, Pian Palù (Fig. 7a), Careser (Fig. 7b) and Santa Giustina) (Fig. 7c) also in good agreement with the observed values. For the Santa Giustina reservoir we eliminated the year 2003, in which it was emptied to allow the construction of a penstock, which diverts the constant MEF of $2.1 \text{ m}^3/\text{s}$ to a small hydropower plant at the toe of the reservoir. The introduction of the MEF modified the monthly releases, such that the simulation has been performed by using two different monthly means for the period pre- and post- introduction of the MEF. In this example the good reproduction

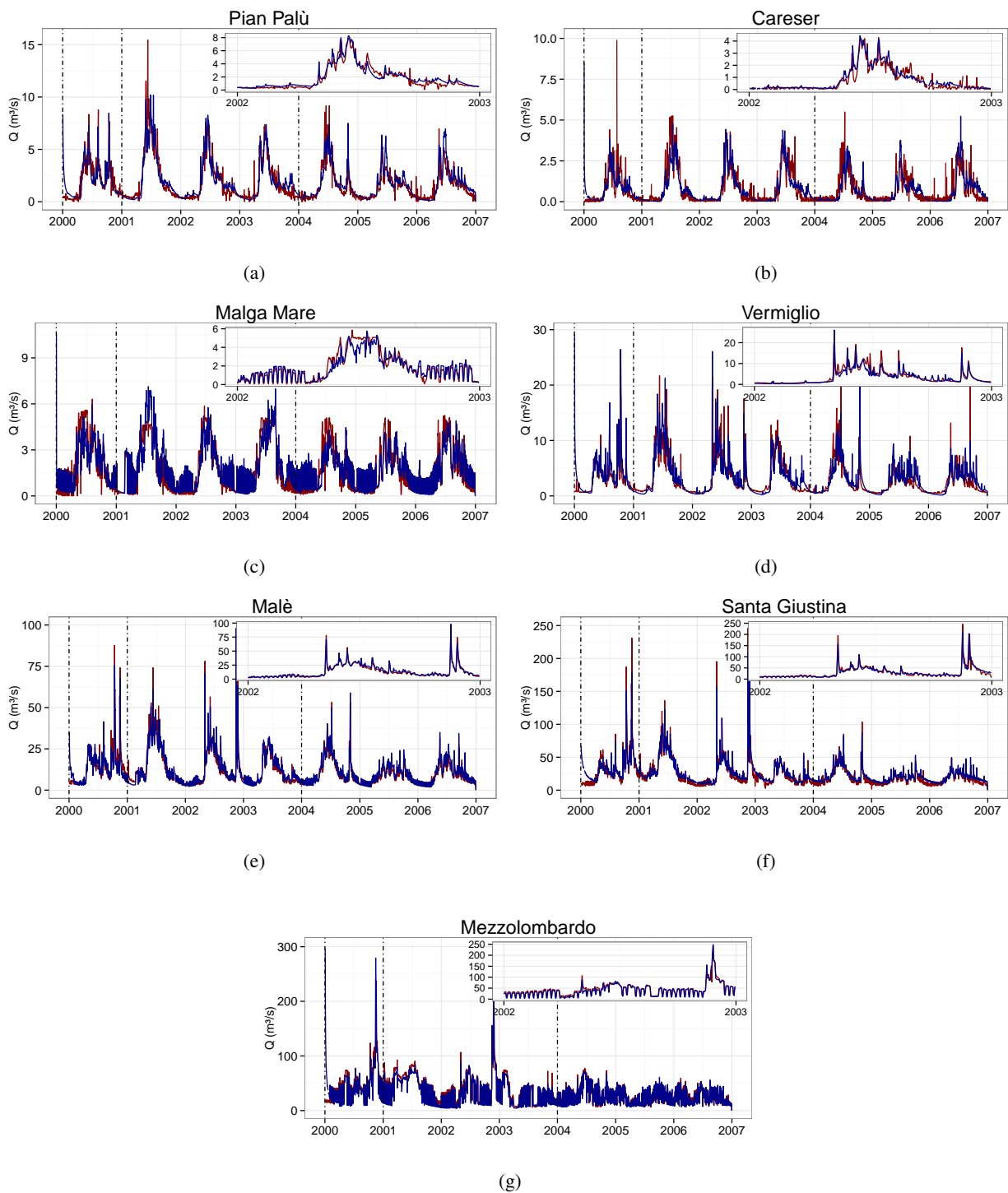


Figure 5: Observed (blue lines) and simulated (red lines) daily streamflows in the period 2000-2006 at the 7 control sections of the Noce river. Dashed vertical lines mark the separation between spin-up, calibration and validation periods. The inset shows a snapshot on year 2002.

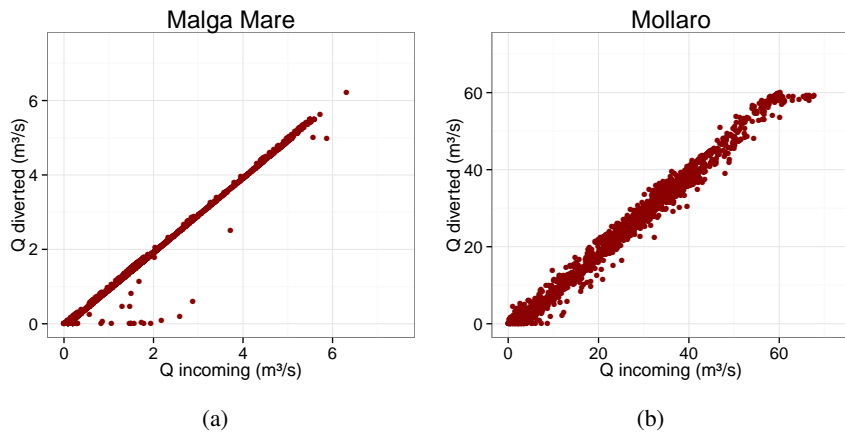


Figure 6: Scatterplots of observed time series of incoming and diverted flows at the reservoirs of a) Malga Mare and b) Mollaro.

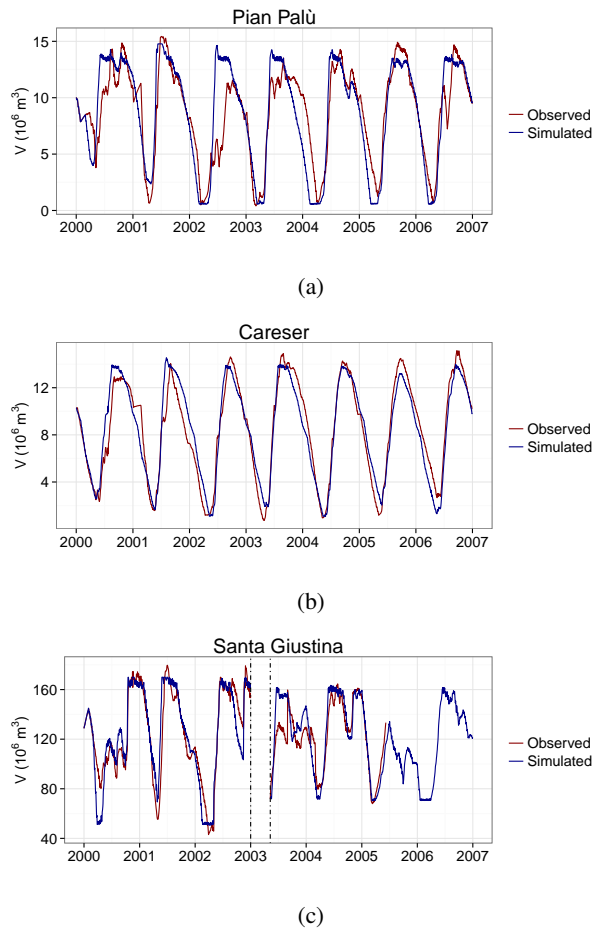


Figure 7: Observed (red line) and simulated (blue line) daily water volumes at a) Pian Palù, b) Careser and c) Santa Giustina reservoirs during the observation period 2000-2006. The part of the graph included between two dashed lines refers to the period in which the Santa Giustina reservoir was emptied.

of streamflow was achieved because of a small variation of the operational rules during the simulation period (2000-2006). Therefore, we do not claim that this approach can be generally applied, and serves only as an example on how operational rules, inferred independently from the hydrological parameters, can be implemented into the model. In fact, we believe that ancillary data whether available can allow a good identification of operational rules. For example, in agricultural reservoirs diverted volumes can be obtained from the irrigation consortia, while for hydropower reservoirs they can be inferred from production data.

Furthermore, Table 6 shows a comparison between observed and simulated average flows from the reservoirs to the connected hydropower plants. With the exception of Santa Giustina before 2003, for which the computed mean diversion flow exceeds of 7.7% the observed mean flow, the percentage differences are always small (less than 2.9 %), thereby indicating that the averaged operational rules are able to match the observed total amount of water transferred for hydropower production reasonably well .

7.4. Scenarios of change

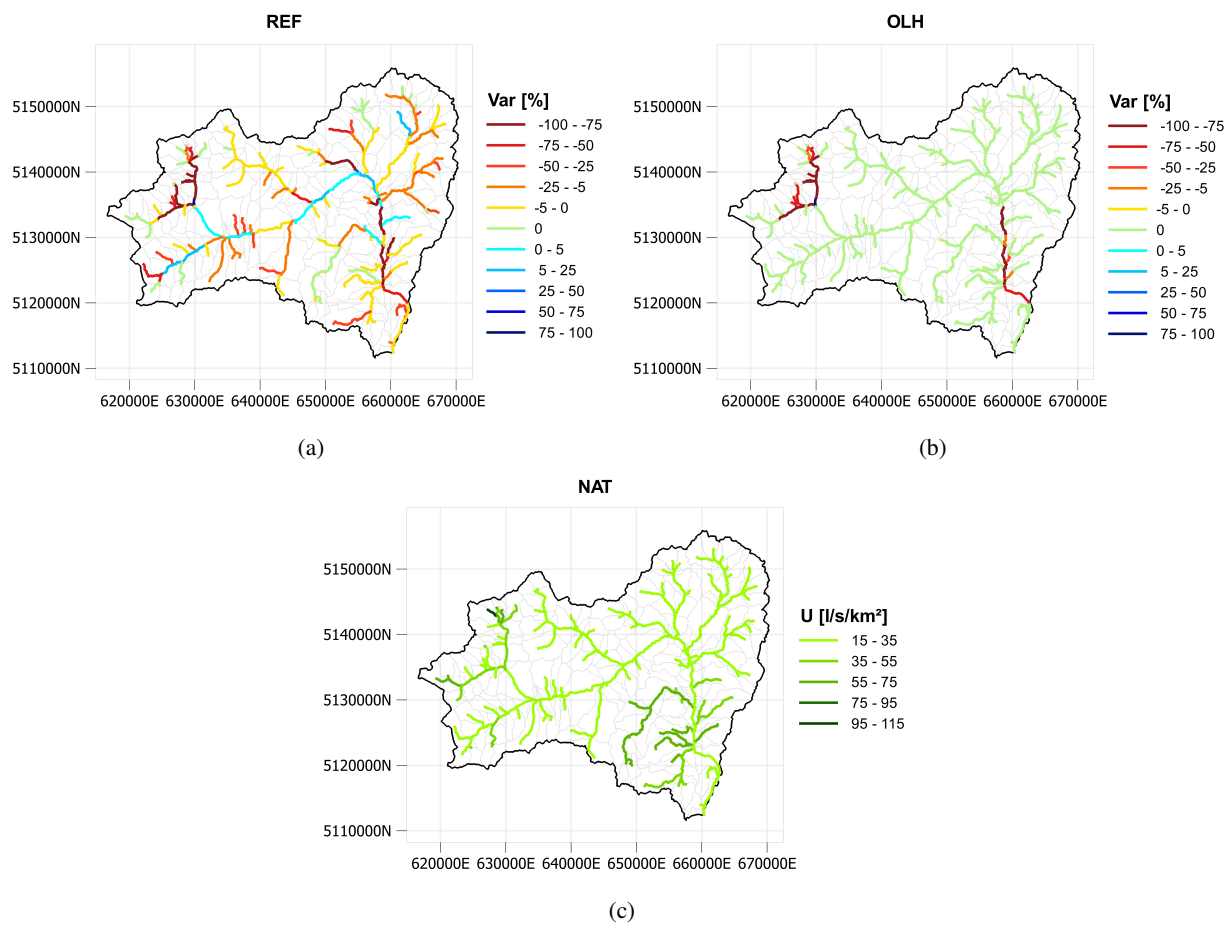


Figure 8: Color maps of the spatial distribution of the percentage relative difference between the average specific discharge u [l/s km²], of a) the REF and the NAT scenarios and b) the OLH and the NAT scenarios. The spatial distribution of u for the NAT period is shown in the panel c). In all cases u has been computed for each stream element as the ratio between average water discharge during the period 2001-2006 and the total drainage area.

In order to demonstrate the ability of the model to deal with catchments experiencing significant streamflow alterations, we propose here a comparison of 3 different scenarios, which have been developed for the Autonomous Province of Trento within a project whose scope was to characterize the hydrological regime of the main rivers of the province. They are: i) the REFerence state of the system (REF), which considers the actual state of the licensed

uses in the catchment as described in Sect. 7.1; ii) a scenario in which Only the reservoirs and the associated Large Hydropower systems are implemented (OLH); and iii) a NATural scenario (NAT) in which all the water uses and hydraulic infrastructures are removed. In particular, the REF scenario is useful for evaluating the spatial variability of the streamflow regime throughout the river basin and for identifying critical areas affected, on average, by low streamflow for prolonged periods of the year. On the other hand, the comparison with OLH scenario may help to identify situations in which hydropower introduces large streamflow alterations. In addition, the NAT scenario reflects the natural system behavior, thus allowing quantification of the alterations to the natural flow regime caused by water uses. Simulations have been performed with the meteorological forcing and water fluxes due to human uses of the period 2000-2006. Finally, model parameter values were those obtained by the calibration on the period 2001-2003 as described in Sect. 7.3.

Fig. 8a shows the actual streamflow alteration computed as the relative difference between the mean specific water discharge u [$l/s km^2$] of REF and NAT scenarios both referred to the period 2001-2006. Fig. 8b repeats Fig. 8a but for the OLH scenario. The specific discharge of the NAT scenario, we used as representative of an ideal condition in which the catchment is free of any human impact, is shown in Fig. 8c. In all cases u is computed as the ratio between mean water discharge of the period of interest and the contributing area. These figures provide a visual perception of the streams within the catchment where the alteration of the natural regime is more severe. In the REF period, alterations in the natural flow regime are distributed through the catchment with 88% of the total river network length (479km) affected. The larger alterations are downstream diversions serving large hydropower plants, but those caused by the other uses are also significant, though of smaller relative magnitude. Positive alterations, i.e. streamflow larger than the natural regime, are observed in streams receiving a contribution from catchments not belonging to their contributing area. With only the large hydropower uses the length of the streams affected by alterations reduces to 12% (Fig. 8b)

Table 6: Observed and simulated average annual flows diverted from the reservoirs to the connected hydropower plant.

| | Observed [m^3/s] | Simulated [m^3/s] | Difference [%] |
|----------------------------|-------------------------|--------------------------|-------------------|
| Pian Palù | 1.66 | 1.65 | -0.6 |
| Careser | 0.71 | 0.71 | 0.0 |
| Malga Mare | 1.90 | 1.92 | 1.1 |
| Santa Giustina before 2003 | 28.40 | 30.58 | 7.7 |
| Santa Giustina after 2003 | 17.53 | 17.03 | -2.9 |
| Mollaro | 23.54 | 22.96 | -2.5 |

These simulations were selected in order to illustrate how GEOTRANSF can be used to create scenarios and evaluate the impact of new derivations, or to evaluate the effects on streamflow of existing uses. It can be used also to develop scenarios combining climate, socio-economic (for what concerns the impact on water resources demand), and land use changes. However, the same type of analysis could have been performed with reference to specific periods in order to identify, for example, critical situations during summer or winter seasons. In addition GEOTRANSF simulations could serve as a tool for river managers supporting the elaboration of scenarios including water uses for which the license has been requested, for example.

8. Conclusions

We present a modeling approach coupling hydrological fluxes with water transfers due to human activities. The tight coupling between hydrological fluxes and water transfers for human use, performed by means of hydraulic infrastructures (channels and reservoirs), is the main novelty of the proposed modeling framework. Irrigation water is taken into account as withdrawal from the stream and applied as recharge to the upper soil bucket of the sub-catchment containing the irrigated area. In case of irrigation water tapped from groundwater, the withdrawal is from the second bucket representing groundwater storage. Reservoirs are included by applying a specific water balance equation with inflow computed by the model considering all the hydrological processes and human interactions occurring upstream. The outflow is divided into two components: the withdrawal for water use and the release downstream, which is given by the sum of the MEF and the spill during flood events. Both outflows depend in a nonlinear manner on

management rules, water elevation in the reservoir (according to the area-capacity curve) and characteristics of the spillways. Given the importance of reservoirs in the management of water resources the model fully exploits this nonlinear relationship and the associated feedbacks avoiding the introduction of simplifications that decouple the two systems, but that may introduce significant errors in modeling their interplay. Hydrological processes are modeled by subdividing the catchment into a given number of sub-catchments connected to the control sections by a network of streams. Each stream receives the contribution from a sub-catchment. This structure allows a better management of the diffuse utilizations than modeling frameworks based on the HRU concept. Small withdrawals from the streams not explicitly modeled (each sub-catchment is composed of hillslopes connected to a sub-network but it is represented as a single element connected to a node of the resolved network) are accounted for in an exact manner evaluating their impact in term of streamflow alteration at the exit of the sub-catchment where it connects to the resolved part of the river network. This is another relevant peculiarity of GEOTRANSF that to our best knowledge is not included in existing modeling approaches. Groundwater withdrawals are grouped at the sub-catchment level with a spatial resolution that can be controlled through the density of the resolved river network. In large basins river network density can vary according to specific needs, for example to better represent complex topography or zones with a large number of groundwater wells and other small withdrawals.

An application showed the flexibility and the accuracy of the model in modeling hydrology in human-modified catchments, while reproducing with accuracy the feedbacks between the hydrological and human systems. GEOTRANSF is also structured in such a way to facilitate the development of scenarios concerning water resources exploitation and in reconstructing streamflow characteristics in the hypothetical case of absence of water uses. This last example can be particularly useful to separate in time series the effect of water uses from that of climate change.

Acknowledgments

This research has been partially funded by the Italian Ministry of Public Instruction, University and Research through the project PRIN 2010-2011 (Innovative methods for water resources management under hydro-climatic uncertainty scenarios, prot. 2010JHF437). We also thank Autonomous Province of Trento and Edmund Mach Foundation for data provision.

Appendix A. Interpolation of meteorological forcing

The spatial distribution of precipitation is obtained by interpolation of the measurements at the available rain gauges by means of either Ordinary Kriging (OK) or Kriging with External Drift (KED) (see e.g., Goovaerts, 1997). The precipitation is interpolated separately at each time step by using the same semivariogram, which should be provided externally. The precipitation is assumed uniformly distributed within the sub-catchments and equal to the value the interpolation provides at the barycenter of the sub-catchment, under the assumption that the correlation length of the precipitation is much larger than the characteristic size of the sub-catchments (Rinaldo et al., 2006). This is a condition not difficult to achieve given that the characteristic size of the sub-catchments can be controlled with the threshold τ_c used for the network extraction, as discussed in Section 2.

Temperature at each time step is computed by linear regression to the values measured at the meteorological stations equipped with temperature sensors with elevation as independent variable. In agreement with the procedure used for the precipitation the temperature assigned to the sub-catchment is computed at its mean elevation.

Appendix B. Snow and Evapotranspiration

Snow accumulation and melting is simulated by using the degree-day model. This model was chosen because at daily time scale, and with air temperature and precipitation as the only input variables, it has been shown to provide results in agreement with more complex models based on energy budget (see e.g., Rango and Martinec, 1995; Beven, 2001; Hock, 2003; Majone et al., 2010). The snow module of GEOTRANSF simulates snow accumulation and melting as a function of air temperature T_a and the following three rules:

$$\begin{aligned}
T_a(t) \leq T_s & \quad \begin{cases} h_s(t) & = h_s(t - \Delta t) + h_p(t) \\ h_{eff}(t) & = 0 \end{cases} \\
T_a(t) \geq T_{sm} & \quad \begin{cases} h_{sm}(t) & = c_m [T_a(t) - T_{sm}] \\ h_s(t) & = h_s(t - \Delta t) - h_{sm}(t) \\ h_{eff}(t) & = h_p(t) + h_{sm}(t) \end{cases} \\
T_s < T_a(t) < T_{sm} & \quad \begin{cases} h_s(t) & = h_s(t - \Delta t) \\ h_{eff}(t) & = h_p(t) \end{cases}
\end{aligned} \tag{B.1}$$

where $h_s(t)$ [L] is the snow water equivalent accumulated at the ground at time t , $h_p(t)$ [L] is the amount of precipitation in the time interval $(t - \Delta t, t]$, $h_{eff}(t)$ [L] is the effective precipitation (sum of rainfall and snowmelt) in the same time interval, T_s and T_{sm} are two threshold temperatures indicating the maximum temperature for precipitation occurring as snow and the minimum temperature for precipitation occurring as rainfall, respectively. In addition, $h_{sm}(t)$ is the amount of melted water in the time interval $(t - \Delta t, t]$ and c_m [$L/^\circ C$] is the melting rate. Notice that when $T_s < T_a < T_{sm}$ precipitation occurs as rainfall, but the energy it adds to the snowpack is not enough to trigger snowmelt.

The daily potential evapotranspiration, ET_p , is computed by multiplying the reference evapotranspiration ET_0 by a crop coefficient K_c which accounts for land use (Allen et al., 1998):

$$ET_p = K_c \cdot ET_0 \tag{B.2}$$

where ET_0 (expressed in mm/day) is computed by using the expression proposed by Hargreaves and Samani (1982):

$$ET_0 = 0.408[0.0023R_a(T_{mean} + 17.8)\sqrt{T_{max} - T_{min}}] \tag{B.3}$$

In Eq. (B.3) T_{mean} , T_{max} and T_{min} are the mean, maximum and minimum daily temperatures, respectively, and R_a is the daily extraterrestrial radiation, which can be computed by using the equations proposed by Duffie and Beckman (1980).

Real evapotranspiration is at its potential limit when soil water content θ is larger than the field capacity θ_{fc} , and it reduces for $\theta < \theta_{fc}$ as an effect of the plant reaction to water stress. To take into account this behavior the following phenomenological relationship is used (see e.g. Rodriguez-Iturbe and Porporato, 2004, ch. 2.1.5):

$$ET_{Real} = \begin{cases} \frac{(\theta - \theta_r)}{(\theta_{fc} - \theta_r)} ET_p & \text{for } \theta_r < \theta < \theta_{fc} \\ ET_p & \text{for } \theta \geq \theta_{fc} \end{cases} \tag{B.4}$$

which assumes that the real evapotranspiration is zero below the residual water content θ_r , when the stomata are assumed to be close, and then it increases linearly to reach the maximum value ET_p for $\theta = \theta_{fc}$. Further increase of soil water content does not change ET_{Real} .

References

- Acreman, M., Overton, I., King, J., Wood, P., Cowx, I., Dunbar, M., Kendy, E., Young, W., 2014. The changing role of ecohydrological science in guiding environmental flows. *Hydrological Sciences Journal* 59 (3-4), 433–450.
- Ahmadi, M., Arabi, M., II, J. C. A., Fontane, D. G., Engel, B. A., 2014. Toward improved calibration of watershed models: Multisite multiobjective measures of information. *Environmental Modelling & Software* 59, 135 – 145.
- Allen, R. G., Pereira, L. S., Raes, D., Smith, M., 1998. Crop evapotranspiration. guidelines for computing crop water requirements. Tech. Rep. Irrigation and drainage Paper nr. 56, FAO - Food and Agriculture Organization of the United Nations, Rome.
- Arnett, R. R., 1971. Slope form and geomorphological process: an australian example. In: *Form and Process*. No. Spec. Publ., 3. London, pp. 81–92.
- Beven, K. J., 2001. *Rainfall-Runoff Modelling: The Primer*. John Wiley & Sons Inc, Chichester.

- Bicknell, B., Imhoff, J., Kittle, J., Donigan, A., Johanson, R., 1997. Hydrological Simulation Program–Fortran HSPF, User’s manual for version 11. Athens, Usa.
URL <http://water.usgs.gov/software/HSPF/>
- Botter, G., Basso, S., Porporato, A., Rodriguez-Iturbe, I., Rinaldo, A., JUN 26 2010. Natural streamflow regime alterations: Damming of the Piave river basin (Italy). *WATER RESOURCES RESEARCH* 46.
- Botter, G., Basso, S., Rodriguez-Iturbe, I., Rinaldo, A., AUG 6 2013. Resilience of river flow regimes. *PNAS* 110 (32), 12925–12930.
- Cao, W., Bowden, W., Davie, T., Fenemor, A., 2006. Multi-variable and multi-site calibration and validation of swat in a large mountainous catchment with high spatial variability. *Hydrological Processes* 20 (5), 1057–1073.
- Castagna, M., Bellin, A., 2009. A bayesian approach for inversion of hydraulic tomographic data. *Water Resour. Res.* 45.
- Chiogna, G., Majone, B., Cano Paoli, K., Diamantini, E., Stella, E., Mallucci, S., Lencioni, V., Zandonai, F., Bellin, A., 2015. A review of hydrological and chemical stressors in the adige catchment and its ecological status. *Science of the Total Environment*.
- Chiogna, G., Santoni, E., Camin, F., Tonon, A., Majone, B., Trenti, A., Bellin, A., 2014. Stable Isotope Characterization of the Vermigliana Catchment. *Journal of Hydrology* 509, 295–305.
- Dalin, C., Konar, M., Hanasaki, N., Rinaldo, A., Rodriguez-Iturbe, I., 2012. Evolution of the global virtual water trade network. *Proceedings of the National Academy of Sciences* 109 (16), 5989–5994.
URL <http://www.pnas.org/content/109/16/5989.abstract>
- Deltares, 2010. RIBASIM (River Basin Simulation Model). Delft, the Netherlands.
URL <https://www.deltares.nl/en/software/ribasim/>
- Destouni, G., Asokan, S., Jarsj, J., 2010. Inland hydro-climatic interaction: Effects of human water use on regional climate. *Geophysical Research Letters* 37 (18).
- Destouni, G., Jaramillo, F., Prieto, C., 2013. Hydroclimatic shifts driven by human water use for food and energy production. *Nature Climate Change* 3 (3), 213–217.
- DHI Software, 2003. A Versatile Decision Support Tool For Integrated Water Resources Management Planning - Guide to Getting Started - Tutorial. Hørsholm, Denmark.
URL <http://www.mikepoweredbydhi.com/products/mike-hydro-basin>
- DHI Software, 2009. MIKE SHE - User Manual. Hørsholm, Denmark.
URL <http://www.mikepoweredbydhi.com/products/mike-she>
- Dietrich, W. E., R. Reiss and, M. L. H., Montgomery, D., 1995. A process-based model for colluvial soil depth and shallow landsliding using digital elevation data. *Hydrological Processes* 9, 383–400.
- Dodov, B., Fofoula-Georgiou, E., 2004a. Generalized hydraulic geometry: Derivation based on a multiscaling formalism. *Water Resour. Res.* 40 (6), W06302.
- Dodov, B., Fofoula-Georgiou, E., 2004b. Generalized hydraulic geometry: Insights based on fluvial instability analysis and a physical model. *Water Resources Research* 40 (12), 1–15.
- Duffie, J. A., Beckman, W. A., 1980. Solar engineering of thermal processes. John Wiley and Sons, New York, USA.
- Dutta, D., Wilson, K., Welsh, W., Nicholls, D., Kim, S., Cetin, L., 2013. A new river system modelling tool for sustainable operational management of water resources. *Journal of Environmental Management* 121, 13–28.
- Efstratiadis, A., Nalbantis, I., Koukouvinos, A., Rozos, E., Koutsoyiannis, D., 2008. HYDROGEIOS: a semi-distributed GIS-based hydrological model for modified river basins. *Hydrol. Earth Syst. Sci.* 12, 989–1006.
- Feldman, A. D., 2000. Hydrologic Modeling System HEC-HMS - Technical Reference Manual. Davis, Usa.
URL <http://www.hec.usace.army.mil/software/hec-hms/documentation.aspx>
- Feller, W., 1971. An Introduction to Probability Theory and Its Applications, 2nd Edition. John Wiley & Sons, New York.
- Formetta, G., Antonello, A., Franceschi, S., David, O., Rigon, R., MAY 2014. Hydrological modelling with components: A GIS-based open-source framework. *Environmental Modelling & Software* 55, 190–200.
- Formetta, G., Mantilla, R., Franceschi, S., Antonello, A., Rigon, R., 2011. The JGrass-NewAge system for forecasting and managing the hydrological budgets at the basin scale: models of flow generation and propagation/routing. *Geosci. Model Dev.* 4 (4), 943–955.
- Fredericks, J., Labadie, J., Altenhofen, J., 1998. Decision support system for conjunctive stream-aquifer management. *Journal of Water Resources Planning and Management* 124 (2), 69–78.
- Goovaerts, P., 1997. Geostatistics for natural resources evaluation. University Press, Oxford, USA.
- Graveline, N., Majone, B., Duiden, R. V., Ansink, E., 2014. Hydro-economic modeling of water scarcity under global change: an application to the Gállego river basin (Spain). *Reg. Environ. Change* 14 (1), 119–132.
- Hargreaves, G. H., Samani, Z. A., 1982. Estimating potential evapotranspiration. *Journal of Irrigation and Drainage Engineering* 108, 225–230.
- Hock, R., 2003. Temperature index melt modelling in mountain areas. *Journal of Hydrology* 282 (1-4), 104–115.
- Kirchner, J. W., Feng, X., Neal, C., 2001. Catchment-scale advection and dispersion as a mechanism for fractal scaling in stream tracer concentrations. *Journal of Hydrology* 254, 82–101.
- La Jeunesse, I., Cirelli, C., Aubin, D., Larrue, C., Sellami, H., Bellin, A., Benabdallah, S., Bird, D., Deidda, R., Dettori, M., Engin, G., Herrmann, F., Ludwig, R., Mabrouk, B., Majone, B., Paniconi, C., Soddu, A., 2015. Is climate change a threat for water uses in the Mediterranean region? Results from a survey at local scale. *Science of The Total Environment*.
URL <http://dx.doi.org/10.1016/j.scitotenv.2015.04.062>
- Labat, D., Mangin, A., Ababou, R., 2000. Rainfall-runoff relations for karstic springs: Part I: Convolution and spectral analyses. *Journal of Hydrology* 238, 123–148.
- Lall, U., 2014. Debates-The future of hydrological sciences: A (common) path forward? One water. One world. Many climes. Many souls. *Water Resources Research* 50 (6), 5335–5341.
URL <http://dx.doi.org/10.1002/2014WR015402>
- Lampert, D., Wu, M., 2015. Development of an open-source software package for watershed modeling with the Hydrological Simulation Program in Fortran. *Environmental Modelling & Software* 68, 166 – 174.

- Leopold, L. B., Maddock, T., 1953. The hydraulic geometry of stream channels and some physiographic implications. U.S. Geol. Surv. Prof. Pap. 252, 57 pp.
- Li, Y., Huang, G., Huang, Y., Zhou, H., 2009. A multistage fuzzy-stochastic programming model for supporting sustainable water-resources allocation and management. *Environmental Modelling & Software* 24 (7), 786 – 797.
- Liu, Y., Gupta, H. V., 2007. Uncertainty in hydrologic modeling: Toward an integrated data assimilation framework. *Water Resources Research* 43 (7), W07401.
- Majone, B., Bellin, A., Borsato, A., 2004. Runoff generation in karst catchments: multifractal analysis. *Journal of Hydrology* 294, 176–195.
- Majone, B., Bertagnoli, A., Bellin, A., 2010. A non-linear runoff generation model in small Alpine catchments. *Journal of Hydrology* 385 (1-4), 300–312.
- Majone, B., Bovolo, C. I., Bellin, A., Blenkinsop, S., Fowler, H. J., 2012. Modeling the impacts of future climate change on water resources for the Gállego river basin (Spain). *Water Resour. Res.* 48, W01512.
- Majone, B., Villa, F., Deidda, R., Bellin, A., 2015. Impact of Climate Change and water use policies on hydropower potential in the south-eastern Alpine region. *Science of The Total Environment*.
URL <http://dx.doi.org/10.1016/j.scitotenv.2015.05.009>
- Michel, C., Andreassian, V., Perrin, C., 2005. Soil Conservation Service Curve Number method: How to mend a wrong soil moisture accounting procedure? *Water Resour. Res.* 41, W02011.
- MRC, 2004. Decision Support Framework, Water Utilisation Project Component A: Final Report. Volume 11: Technical Reference Report, DSF 620 SWAT and IQQM Models. Phnom Penh, Cambodia.
- Nalbantis, I., Efstratiadis, A., Rozos, E., Kopsiafti, M., Koutsoyiannis, D., 2011. Holistic versus monomeric strategies for hydrological modelling of human-modified hydrosystems. *Hydrology and Earth System Sciences* 15 (3), 743–758.
- Nazemi, A., Wheeler, H., 2015a. On inclusion of water resource management in earth system models -part 1: Problem definition and representation of water demand. *Hydrology and Earth System Sciences* 19 (1), 33–61.
- Nazemi, A., Wheeler, H., 2015b. On inclusion of water resource management in earth system models part 2: Representation of water supply and allocation and opportunities for improved modeling. *Hydrology and Earth System Sciences* 19 (1), 63–90.
- Neitsh, S. L., Arnold, J. G., Kiniry, J. R., Williams, J. R., 2011. Soil and water assessment tool: Theoretical documentation version 2009. Tech. Rep. TR406-2011, Texas A&M University, Texas Water Resources Institute, College Station, Texas 77843-2118.
- O'Callaghan, J., Mark, D., 1984. The extraction of drainage networks from digital elevation data. *Computer Vision, Graphics, & Image Processing* 28 (3), 323–344.
- Orlandini, S., 2002. On the spatial variation of resistance to flow in upland channel networks. *Water Resources Research* 38 (10), 151–1514.
- Orlandini, S., Boaretti, C., Guidi, V., Sfondrini, G., 2006. Field determination of the spatial variation of resistance to flow along a steep alpine stream. *Hydrological Processes* 20 (18), 3897–3913.
- Orlandini, S., Moretti, G., Franchini, M., Aldighieri, B., Testa, B., 2003. Path-based methods for the determination of nondispersive drainage directions in grid-based digital elevation models. *Water Resources Research* 39 (6), TNN11–TNN18.
- Orlandini, S., Moretti, G., Gavioli, A., 2014. Analytical basis for determining slope lines in grid digital elevation models. *Water Resources Research* 50 (1), 526–539.
- PGUAP, 2006. Piano generale di utilizzazione delle acque pubbliche. Trento.
URL <http://pguap.provincia.tn.it/>
- Piccolroaz, S., Majone, B., Palmieri, F., Cassiani, G., Bellin, A., 2015. On the use of spatially distributed, time-lapse microgravity surveys to inform hydrological modeling. *Water Resources Research*.
URL <http://dx.doi.org/10.1002/2015WR016994>
- Planchon, O., Darboux, F., 2001. A fast, simple and versatile algorithm to fill the depressions of digital elevation model. *Catena* 46, 159–176.
- Rango, A., Martinec, J., 1995. Revisiting the degree-day method for snowmelt computations. *Water Resources Bulletin* 31 (4), 657–669.
- Rinaldo, A., Botter, G., Bertuzzo, E., Uccelli, A., Settini, T., Marani, M., 2006. Transport at basin scales: 1. Theoretical framework. *Hydrol. Earth Syst. Sci.* 10 (1), 19–29.
- Robinson, J., Rahmat-Samii, Y., 2004. Particle Swarm Optimization in Electromagnetics. *Ieee Transactions on antennas and propagation*. *Ieee Transactions on antennas and propagation* 52 (2), 397–407.
- Rodriguez-Iturbe, I., Porporato, A., 2004. *Ecology of water-controlled ecosystems. Soil moisture and plant dynamics*. Cambridge University Press, Cambridge, UK.
- Rodriguez-Iturbe, I., Rinaldo, A., 1997. *Fractal river basins: Chance and self-organization*. Cambridge University Press, Cambridge, UK.
- Rodriguez-Iturbe, I., Valdes, J., 1979. The geomorphologic structure of hydrologic response. *Water Resour. Res.* 15 (6), 1409–1420.
- Ross, B., Contractor, D., Shanholtz, V., 1979. A finite-element model of overland and channel flow for assessing the hydrologic impact of land-use change. *Journal of Hydrology* 41 (1-2), 11 – 30.
URL <http://www.sciencedirect.com/science/article/pii/002216947990101X>
- Rubin, Y., Chen, X., Murakami, H., Hahn, M., 2010. A bayesian approach for inverse modeling, data assimilation, and conditional simulation of spatial random fields. *Water Resour. Res.* 46 (9).
- Savenije, H. H. G., Hoekstra, A. Y., van der Zaag, P., 2014. Evolving water science in the anthropocene. *Hydrology and Earth System Sciences* 18 (1), 319–332.
URL <http://www.hydrol-earth-syst-sci.net/18/319/2014/>
- Seekell, D. A., D'Odorico, P., Pace, M. L., APR-JUN 2011. Virtual water transfers unlikely to redress inequality in global water use. *Environmental Research Letters* 6 (2).
- Simons, M., Podger, G., Cooke, R., 1996. Iqqm - a hydrologic modelling tool for water resource and salinity management. *Environmental Software* 11 (1-3), 185–192.
- Sivapalan, M., Savenije, H. H., Blöschl, G., 2012. Socio-hydrology: A new science of people and water. *Hydrol. Process.* 26 (24), 1270–1276.
- Tarboton, D. G., 1997. A new method for the determination of flow directions and upslope areas in grid digital elevation models. *Water Resources Research* 33 (2), 309–319.

- URL <http://dx.doi.org/10.1029/96WR03137>
- Thompson, S. E., Sivapalan, M., Harman, C. J., Srinivasan, V., Hipsey, M. R., Montanari, A., Blöschl, G., 2013. Developing predictive insight into changing water systems: use-inspired hydrologic science for the Anthropocene. *Hydrol. Earth Syst. Sci.* 17, 5013–5039.
- Traynham, L., Palmer, R., Polebitski, A., 2011. Impacts of future climate conditions and forecasted population growth on water supply systems in the puget sound region. *Journal of Water Resources Planning and Management* 137 (4), 318–326.
- U.S. Soil Conservation Service, 1964. *Scs national engineering handbook*. Washington D.C.
- Vrugt, J. A., Gupta, H. V., Bouten, W., Sorooshian, S., 2003. A shuffled complex evolution metropolis algorithm for optimization and uncertainty assessment of hydrologic model parameters. *Water Resources Research* 39 (8).
- URL <http://dx.doi.org/10.1029/2002WR001642>
- Welsh, W., Vaze, J., Dutta, D., Rassam, D., Rahman, J., Jolly, I., Wallbrink, P., Podger, G., Bethune, M., Hardy, M., Teng, J., Lerat, J., 2013. An integrated modelling framework for regulated river systems. *Environmental Modelling and Software* 39, 81–102.
- Yates, D., Sieber, J., Purkey, D., Huber-Lee, A., 2005. Weap21 - a demand-, priority-, and preference-driven water planning model. part 1: Model characteristics. *Water International* 30 (4), 487–500.
- Zagona, E., Fuip, T., Shane, R., Magee, T., Goranflo, H., 2001. Riverware: A generalized tool for complex reservoir system modeling. *Journal of the American Water Resources Association* 37 (4), 913–929.
- Zolezzi, G., Bellin, A., Bruno, M. C., Maiolini, B., Siviglia, A., DEC 29 2009. Assessing hydrological alterations at multiple temporal scales: Adige River, Italy. *WATER RESOURCES RESEARCH* 45.